AD-A264 623

MENTATION PAGE

OMB No. 0704-0188

REPORT DATE	3. REPORT TYPE AND DATES COVERED
	FINAL/01 FEB 92 TO 31 JAN 93

4. TITLE AND SUBTITLE

"MULTISCALE AND MULTIGRID INFORMATION REPRESENTATION, EXTRACTION AND FUSION" (U)

5. FUNDING NUMBERS

2304/ES
F49620-92-J-0134

6. AUTHOR(S)

Dr Ahmed Tewfik

7. PERFORMING ORGANIZATION NAME(S) AND ADDRESS(ES)

University of Minnesota
Electrical Engineering
Minneapolis MN 55455

8. PERFORMING ORGANIZATION REPORT NUMBER

AFOSR-TR- 93 0014

9. SPONSORING MONITORING AGENCY NAME(S) AND ADDRESS(ES)

AFOSR/NM
110 DUNCAN AVE, SUTE B115
BOLLING AFB DC 20332-0001

10. SPONSORING MONITORING AGENCY REPORT NUMBER

F49620-92-J-0134

DTIC
ELECTE
MAY 21 1993
S A D

11. SUPPLEMENTARY NOTES

12a. DISTRIBUTION AVAILABILITY STATEMENT

APPROVED FOR PUBLIC RELEASE: DISTRIBUTION IS UNLIMITED

12b. DISTRIBUTION CODE

UL

13. ABSTRACT (Maximum 200 words)

The basic goal of this research was to study the role that wavelet theory can play in information representation and extraction. The researchers focused their attention primarily on surveillance applications. As part of their research, they studied two problems that arise in surveillance. The first problem was that of determining the directions of arrivals of a set of plane waves in the presence of a background noise of unknown correlarion structure. The second problem involved selecting an optimal set of N waveforms, with N fixed, to obtain the best reconstruction of a distributed range-Doppler target reflectivity function.

93 5 20 020

93-11311

14. SUBJECT TERMS

15. NUMBER OF PAGES
36

16. PRICE CODE

17. SECURITY CLASSIFICATION OF REPORT	18. SECURITY CLASSIFICATION OF THIS PAGE	19. SECURITY CLASSIFICATION OF ABSTRACT	20. LIMITATION OF ABSTRACT
UNCLASSIFIED	UNCLASSIFIED	UNCLASSIFIED	SAR(SAME AS REPORT)

April 1993

Multiscale and Multigrid Information Representation, Extraction and Fusion

Final Technical Report

Principal Investigator
Dr. Ahmed H. Tewfik

Program Manager
Dr. Jon Sjogren

Sponsored by
Air Force Office of Scientific Research
Grant No. AF/F49620-92-J-0134

Department of Electrical Engineering
University of Minnesota
Room 4-174 EE/CSci. Bldg.
Minneapolis, MN 55455

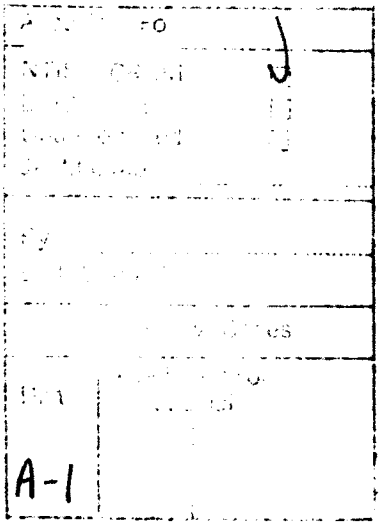

Contents

1 SUMMARY

This report briefly describes the research carried out by faculty and graduate students of the Department of Electrical Engineering at the University Minnesota under grant AFOSR AF/F49620-92-J-0134. The principal investigator for this research was Prof. Ahmed H. Tewfik. The period covered in this report is February 1, 1992 to January 31, 1993.

The basic goal of this grant was to study the role that wavelet theory can play in information representation and extraction. We focused our attention primarily on surveillance applications. As part of our research, we studied two problems that arise in surveillance. The first problem was that of determining the directions of arrivals of a set of plane waves in the presence of a background noise of unknown correlarion structure. The second problem involved selecting an optimal set of N waveforms, with N fixed, to obtain the best reconstruction of a distributed range-Doppler target reflectivity function.

We established that the correlation structures of the wavelet transforms of the outputs of an array of sensors due to plane waves and these due to wide classes of background noise are different. We constructed a method that exploits these differences to estimate the directions of arrival of the plane waves. We also demonstrated the feasibility of this approach and its superiority over traditional approaches using numerical simulations.

We showed that the most accurate reconstruction of a range-Doppler target density that can be computed from N waveforms and their echoes is obtained by transmitting the singular functions corresponding to the N largest singular values of two kernels derived from the target density. The singular functions are valid wavelets that obey an additional orthogonality constraint in the frequency domain. Using this result, we proposed a solution to the problem of choosing a set of N waveforms to reconstruct with high accuracy an arbitrary unknown target range-Doppler density function.

We also studied two signal representation problems. Specifically, we investigated the completeness of an arbitrary sampling of a redundant dyadic wavelet transform. We gave a necessary and sufficient condition for the completeness of any such representation of any discrete time or space finite data length signal (including dyadic wavelet transform extrema and zero-crossings representations). We showed that completeness depends only on the locations of the retained samples of the dyadic wavelet transform. Our completeness test is more convenient and easier to verify than previously derived tests. Furthermore, we explained why some conclusions reported in the literature hold for most signals except for some extreme cases. We showed how to ensure the completeness of the representation by adding additional information in those cases where the sampled dyadic wavelet transform domain representation is incomplete. We also studied the numerical stability of such a representation. The stability issue is important in the sense that a numerically unstable representation is useless from a practical point of view. We described a fast fast Fourier transform (FFT) based recon-

struction algorithm from such a signal representation. This work is important in that it provides us with the theoretical tools that we need to further study efficient and highly adaptive signal representations. Such representations can lead to fast processing algorithms and more powerful signal coding algorithms.

Finally, we studied another wavelet based signal representation procedure. Our aim was to understand how discrete orthogonal non-redundant wavelet representations (as opposed to the redundant dyadic representations mentioned above) can be adapted to a given problem by minimizing a cost function (e.g., bit rate in coding or number of flops required to implement a detector in radar detection) subject to satisfying a second constraint (e.g., the quality of the encoded waveform or a fixed probability of detection and a maximal probability of false alarm). We chose to study this problem in the context of high quality low bit rate audio coding. Our results extend however to other similar problems, e.g., the design of near-optimal radar waveform detectors of minimal complexity. We showed that the regularity property of wavelets is important in coding applications. We also established that adapting the selection of the analysis wavelet to the underlying signal can lead to great reductions in bit rate. Our main contribution was to construct a procedure that exploits the masking effect in human hearing by properly choosing the analysis wavelet in a dynamic and adaptive manner. Our procedure has lead to a high quality audio compression procedure that, for a given quality, can achieve lower bit rates than the MPEG audio standard.

In the following section, we present a brief introduction to wavelet theory. Next, we summarize the results that we have obtained. A list of publications supported in part by this grant is also included.

We are continuing our research in the areas discussed in this report with funding from AFOSR under grant AF/F49620-93-1-0151DEF.

2 WAVELET TRANSFORMS

2.A Introduction

Signal transforms have become a powerful tool in system theory and signal processing. In a typical transform, a signal of interested is expressed as a weighted superposition of a countably infinite set of basis functions ("discrete transforms") or as a weighted integral of a particular function ("continuous transforms") Examples of discrete transforms of include Fourier series expansions of periodic functions and Karhunen-Loeve representations of stochastic processes over a finite interval. The best known continuous transform is of course the continuous time Fourier transform.

While known transforms are extremely useful in various applications (e.g., Fourier transforms are the basis of system and modulation theories, Karhunen-Loeve expansions are used in pattern recognition and detection and estimation theories) they do suffer from a number of disadvantages when applied to certain problems. For example, the computation of a Karhunen-Loeve expansion is an expensive operation as it involves solving an eigenvalue-eigenfunction (vector) problem. Furthermore, most transforms yield information about the signal which is *not localized* in time, e.g. the Fourier transform or coefficient of a signal does depend on the value of the signal over its entire support. This implies that coefficients may be wasted to represent the signal over intervals where it is identically zero, transforms change if the support of the signal changes or more data is acquired and it is difficult to relate the local behavior of a signal to its transform.

To address the above mentioned drawbacks, researchers have recently proposed the *wavelet transform* as a fast technique for studying the local behavior of a signal[1]. The idea behind this new transform is that if one wants to study the local behavior of a signal, one has to implicitly window the signal and focus on the resulting signal slice. Short windows will of course lead to high resolution in the time domain and lower resolution in the frequency domain. On the other hand, long windows provide high resolution in the frequency domain and low resolution in the time domain. To gain a certain degree of freedom in trading time versus frequency resolution one may then want to use windows of different support lengths. However, such windows should be properly constructed to enable the user to relate the results obtained with the various analysis windows. The solution adopted in wavelet transforms is to use dilates of a single properly constructed window.

This section is organized as follows. We begin with a review of continuous wavelet transforms. The focus in that sub-section is on the ability of the wavelet transform to trade time and frequency resolutions in a specified manner. This property of the wavelet transform is emphasized in applications that require

[1] Although the formalization of the wavelet transform and the study of its properties is new, the idea behind it is not new. See, e.g. [9], [10].

time-frequency representations of an underlying signal. We then shift our attention to discrete orthogonal wavelet transforms. This class of transforms is non-redundant and has been found to be most useful in signal processing applications. In particular, we will discuss the construction of discrete orthogonal wavelets and the computation of the discrete orthogonal wavelet transform of a given signal. We will emphasize in that part of Section 2 the issue of regularity of the analyzing wavelet and the effect of that regularity on the structure of the wavelet transform of broad classes of signals.

2.B Continuous Wavelet Transform

In a continuous wavelet transform, one attempts to express the signal $f(t)$ in terms of translates of dilates of a single function $\psi(t)$ where the weight given to each translate and dilate is proportional to the inner product between $f(t)$ and that particular translate or dilate. Assuming for the moment that $f(t)$ has finite energy and that $\psi(t)$ is a suitable wavelet function then $f(t)$ can be written as [25], [37]

$$f(t) = \frac{1}{C_\psi} \int_{\infty}^{\infty} \int_{0}^{\infty} \sqrt{s} F(s,u) \psi(s(t-u)) du ds \qquad (2.B.1)$$

where C_ψ is a finite constant and $F(s,u)$ is the wavelet transform of $f(t)$ and is given by

$$F(s,u) = \sqrt{s} \int_{\infty}^{\infty} f(t) \psi(s(t-u)) dt. \qquad (2.B.2)$$

The variable s in the above equations is the "*scale*" variable because it controls the effective width of the support of $\psi(t)$. The variable "u" has the dimension of time and gives the amount by which $\psi(st)$ has been translated in the time domain.

Since (2.B.1) must hold for any finite energy signal $f(t)$, $\psi(t)$ cannot be an arbitrary function. By taking the Fourier transform of both sides of (2.B.1) it becomes clear that we must have

$$\int_{0}^{\infty} \frac{|\Psi(\frac{\omega}{s})|^2}{s} ds > 0 \qquad \forall \omega, \qquad (2.B.3)$$

where $\Psi(\omega)$ denotes the Fourier transform of $\psi(t)$. (Otherwise we may not be able to represent functions that have energies at frequencies where the integral in the above equation is zero.) In fact, the wavelet $\psi(t)$ is chosen such that

$$0 < C_\psi = \int_{0}^{\infty} \frac{|\Psi(\frac{\omega}{s})|^2}{s} ds < \infty. \qquad (2.B.4)$$

Note that by making a change of variable of integration in (3.4) we may also express C_ψ as

$$C_\psi = \int_{0}^{\infty} \frac{|\Psi(\omega)|^2}{\omega} d\omega. \qquad (2.B.5)$$

Eqs. (3.4) and (2.B.5) implies that $\Psi(\omega)$ is zero at $\omega = 0$ and must decay fast enough as ω tends to 0. This is condition is intuitively pleasing: the only frequency that is not affected by division by the scale s is $\omega = 0$. If $\Psi(0) \neq 0$ then all dilates of $\psi(t)$ would contribute to DC ($\omega = 0$) leading to an infinite concentration of energy at $\omega = 0$.

By using (2.B.5) one can also show [25] that the wavelet transform is energy preserving, i.e. one can establish the following "Parseval Theorem" like result

$$\int_0^\infty \int_{-\infty}^\infty |F(s,u)|^2 ds du = C_\psi \int_{-\infty}^\infty |f(t)|^2 dt. \tag{2.B.6}$$

Equation (2.B.5) provides a "recipe" for constructing wavelet functions $\psi(t)$. Specifically, to construct a wavelet $\psi(t)$ one can start with any finite energy function $\phi(t)$ such that its Fourier transform $\Phi(\omega)$ is bounded and decays to zero faster than ω^{p+1} for some integer p as ω tends to infinity. One can then take $\Psi(\omega) = (j\omega)^p \Phi(\omega)$. This is illustrated in Fig. 1 where we have chosen $\phi(t)$ to be a zero-mean Gaussian function of variance equal to unity and the corresponding $\psi(t)$ is taken to be the second derivative of the Gaussian, a choice that is popular in the computer vision literature.

Note that wavelets constructed using the above recipe will have p zeros at $\omega = 0$ and hence will have p vanishing moments, i.e.,

$$\int_{-\infty}^\infty t^m \psi(t) dt = 0, \qquad m = 0, 1, 2, \cdots, p-1. \tag{2.B.7}$$

This in turn implies that if the signal $f(t)$ is smooth enough then

$$|F(s,u)| < C \frac{1}{s^p} \tag{2.B.8}$$

for some finite constant C that depends on $\psi(t)$ and $f(t)$. Thus, for such smooth signals, most of the energy in $F(s,u)$ will appear at lower scales.

Now let us assume without loss of generality that the support of $\psi(t)$ is centered around the origin. Denote by σ_t^2 the variance of $\psi(t)$ in the time domain, i.e.

$$\sigma_\psi^2 = \frac{\int_{-\infty}^\infty t^2 \psi^2(t) dt}{\int_{-\infty}^\infty \psi^2(t) dt}. \tag{2.B.9}$$

Furthermore, assuming that $\psi(t)$ is real we have $|\Psi(\omega)| = |\Psi(-\omega)|$. Denote by $\overline{\omega}$ and σ_ω^2 the center of the pass- band of the Fourier transform $\Psi(\omega)$ of $\psi(t)$ in the frequency domain and its variance around $\overline{\omega}$, i.e.

$$\overline{\omega} = \frac{\int_0^\infty \omega |\Psi(\omega)|^2 d\omega}{\int_0^\infty |\Psi(\omega)|^2 d\omega} \tag{2.B.10}$$

$$\sigma_\psi^2 = \frac{\int_0^\infty (\omega - \overline{\omega})^2 |\Psi(\omega)|^2 d\omega}{\int_0^\infty |\Psi(\omega)|^2 d\omega} \tag{2.B.11}$$

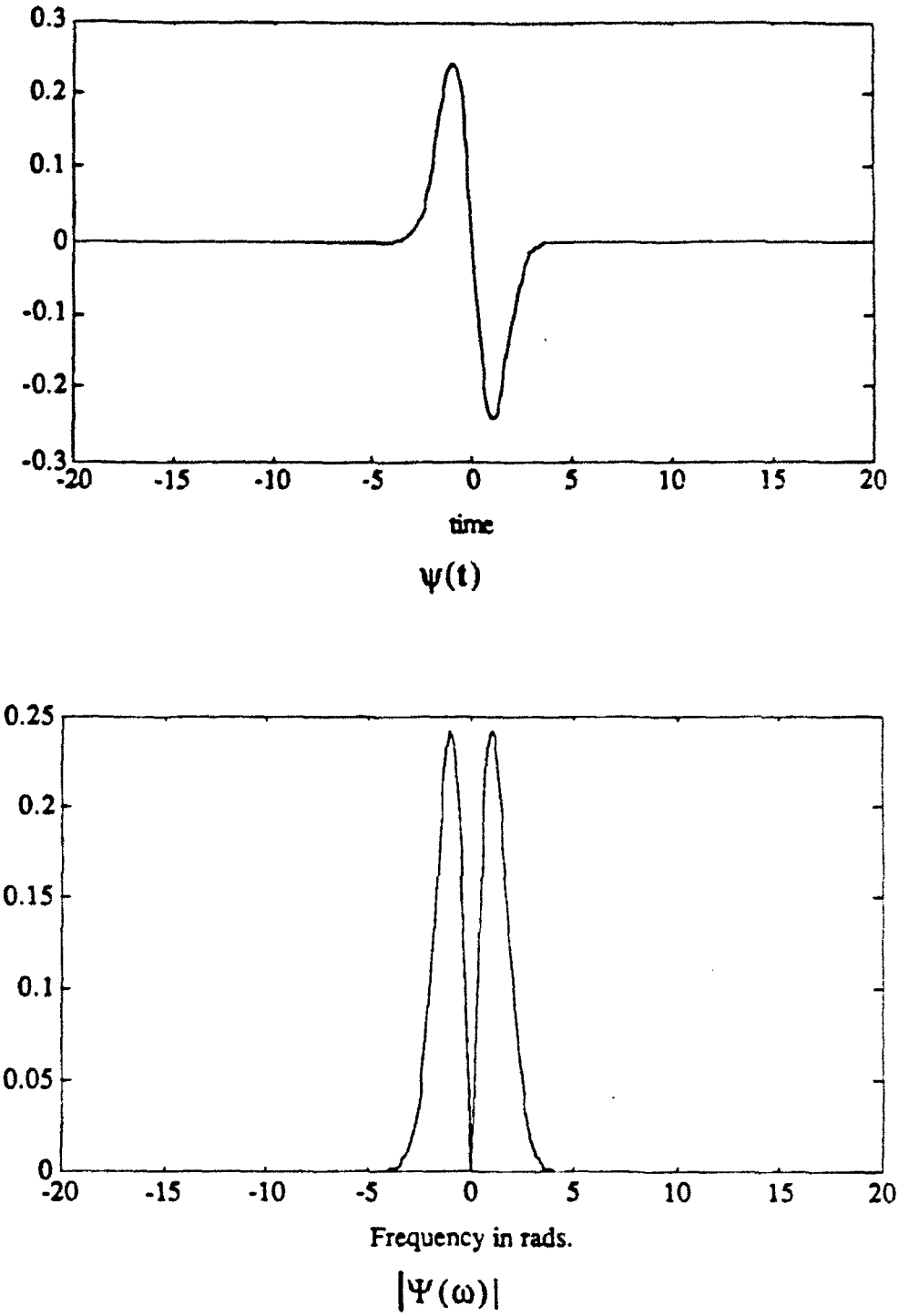

Figure 1: Example of a wavelet function

Clearly, $F(s,u)$ is mainly affected by the behavior of $f(t)$ in the time interval $[u-2\sigma_t/s, u+2\sigma_t/s]$. On the other hand, by Parseval's theorem, $F(s,u)$ may also be rewritten as

$$F(s,u) = \frac{1}{2\pi}\int \mathcal{F}(\omega)\Psi^*(\frac{\omega}{s})e^{-j\omega u}d\omega, \qquad (2.B.12)$$

where $\mathcal{F}(\omega)$ denotes the Fourier transform of $f(t)$. Hence, $F(s,u)$ is also mainly affected by the behavior of $\mathcal{F}(\omega)$ in the time interval $[s(\overline{\omega}-2\sigma_\omega), s(\overline{\omega}+2\sigma_\omega)]$. In particular, for large values of s, $F(s,u)$ carries information about $f(t)$ that is essentially localized in the time domain whereas for small values of s, it carries information about $\mathcal{F}(\omega)$ that is localized in the frequency domain.

Observe also that the wavelet transform (2.B.1) is effectively a mapping from 1- D functions to 2-D functions. Since there is no one-to-one correspondence between all 1- D finite energy and all 2-D finite energy functions, we should expect $F(s,u)$ to be redundant, i.e. to actually be in a subspace of all finite energy 2-D functions. This turns out to be the case. In particular it may be shown that any valid wavelet transform $F(s,u)$ must be left invariant by the application of a particular operator with kernel $K(s,s';u,u')$, e.g.,

$$F(s',u') = \int_{\infty}^{\infty}\int_{0}^{\infty} F(s,u)K(s,s';u,u')duds \qquad (2.B.13)$$

where the non-invertible operator $K(s,s';u,u')$ is given by

$$K(s,s';u,u') = \frac{1}{C_\psi}\int_{\infty}^{\infty} dt\sqrt{ss'}\psi(s'(t-u'))\psi(s(t-u)). \qquad (2.B.14)$$

While in general signal processing applications this redundancy may not be desirable, it may be useful in certain applications.

In the next subsection we shall derive a non-redundant wavelet transform by sampling $F(s,u)$ on an appropriate grid for a more restricted class of wavelets $\psi(t)$. The advantages of using the redundant transform developed here over the non-redundant one are that one can use wavelets from a much wider class and that one can tolerate larger quantization or round-off errors in representing $F(s,u)$ while guaranteeing that the reconstructed signal $f(t)$ has a relative error of norm smaller than that in the quantized version of $F(s,u)$. A complete theory of redundant representation similar to the continuous transform given here is described in [18].

Fig. 2.b illustrates the wavelet transform of the function $f(t)$ given in Fig. 2.a computed with respect to a wavelet with five vanishing moments. Note that the local extrema of the wavelet transform at the various scales correspond to points of discontinuity of the function $f(t)$ or of its derivative. This can be easily explained as follows. Let us assume for simplicity that the support of $\psi(t)$ is finite and that $\psi(t)$ has p vanishing moments. Let us also assume that away from its points of discontinuity the signal $f(t)$ is a piece-wise smooth function.

In particular, we assume that we can expand $f(t)$ in the neighborhood of $t = u_0$ between two points of discontinuities of $f(t)$ in a p- term Taylor series expansion. Now note that for large values of the scale parameter "s" the support of $\psi(st)$ will be small and $F(s,u)$ will be determined by the values of $f(t)$ around the point u_0. In particular, if we substitute the p-term Taylor series expansion of $f(t)$ in the integral that defines $F(s,u)$ and use the fact that $\psi(t)$ has p vanishing moments we find that $|F(s,u)|$ will decay at the rate of $1/s^p$ in the vicinity of $u = u_0$. On the other hand, if the neighborhood of size equal to the support of $\psi(st)$ around $u = u_0$ contains points where $f(t)$ is not smooth enough then this rate of decay will not hold.

The fact that extrema of wavelet transforms correspond to points of discontinuity of $f(t)$ has been used in [38] to register signals. It is also shown experimentally in that reference that certain types of signals can be reconstructed from the extrema of their wavelet transforms. We will discuss this point further in the next section.

2.C Sampling the Wavelet Transform

As mentioned above, a valid wavelet transform $F(s,u)$ is left invariant by the application of the kernel $K(s,s';u,u')$. This is similar to bandlimited signals which are also left invariant by ideal low pass filtering.

The redundancy present in a bandlimited signal can be exploited to obtain more efficient representations of the signal [72]. For example, a familiar result is the a bandlimited signal is uniquely determined by its samples taken on a suitable grid. Similarly, it is by now well known that almost all bandpass signals of bandwidth less than one octave can also be constructed from their zero-crossings [35].

It is natural to ask whether one can exploit the redundancy in a wavelet transform in order to derive more efficient transforms. The answer to this question turns out to be yes. We will discuss one such possibility in this section based on the extrema of the wavelet transform. In the next section, we discuss another non-redundant representation that is based on a judicious sampling of the continuous wavelet transform.

2.C.1 Reconstruction of a Wavelet Transforms from Its Extrema

As mentioned above, Logan [35] has shown that any signal $f(t)$ that does not share any zero crossings with its Hilbert transform can be reconstructed from its zero crossings. Now recall that the wavelet transform of a signal $f(t)$ at a given scale fixed scale s may be interpreted as the output of a filter of impulse response $\psi(-st)$ driven by $f(t)$. It then follows from Logan's results that if $\Psi(\omega)$ is chosen to be non-zero only over the interval $\pi \leq |\omega| \leq 2\pi$ for example, $F(s,u)$ can be reconstructed at each scale s from its zero crossings.

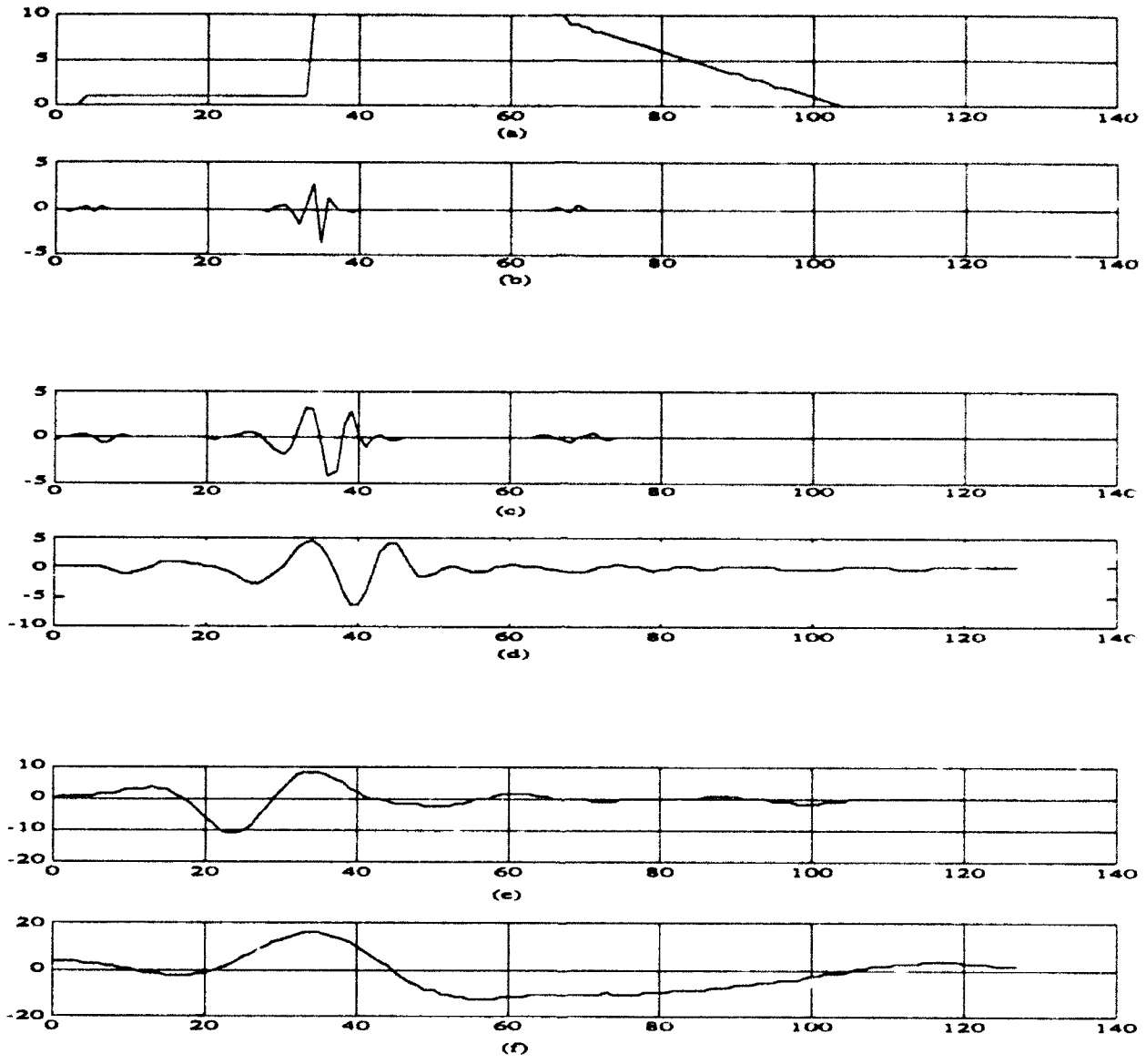

Figure 2: Example of a continuous wavelet decomposition. The original signal is shown in Fig. 2.a. The wavelet transform at various scales is shown in Figs. 2.b-2.f. Fig. 2.b corresponds to the finest scale and 2.f to the coarsest scale.

Unfortunately the above characterization is unstable in that a small error in the actual location of the zero crossings may lead to large errors in the reconstructed function $F(s,u)$. Furthermore, it is difficult to relate the location of the zero crossings of $F(s,u)$ to the local behavior of $f(t)$ when $\Psi(\omega)$ is chosen as above.

The latter difficulty may be circumvented by picking wavelets that have a large number of vanishing moments. It is then possible to relate the rate of decay of $F(s,u)$ to the local behavior of $f(t)$ (and in particular its local regularity as captured by its local Lipschitz exponent [28]). To stabilize the reconstruction several researchers in computer vision have suggested using additional information such as the gradient of the wavelet transform [27] or the value of the integral of the wavelet transform between two consecutive crossings [38].

Motivated by the fact that in practice only samples of the signal $f(t)$ are available for processing, Mallat [38] has also formulated a discrete signal reconstruction problem in which the goal is to reconstruct an $N = 2^J$ point discrete time sequence from the extrema of its wavelet transform at scales 2^j, $j = 0, 1, \cdots, J-1$ and its approximation at scale 1. (The given partial wavelet information is not necessarily complete, i.e. it need not correspond to a unique signal.) An iterative algorithm is given in that same reference for solving this problem. The algorithm performs a sequence of alternating projections onto the set of valid wavelet transforms and that of 2-D functions that have the given extrema. It was shown to converge experimentally but no theoretical proof of its convergence was given.

A second iterative algorithm for solving this problem was presented in [11]. This algorithm differs from that of [38] in its choice of the sets onto which projections are performed. In particular, the sets it uses are closed and convex a property that guarantees the convergence of the algorithm. We will discuss this problem further in Section 3.C where we describe our research in the area of sampling dyadic wavelet transforms.

The practical importance of the results described above is that they pave the way for the development of novel techniques for separating mixed signals. Specifically, it may be possible to separate two signals from an observation of their sum as long as the two signals have different local Lipschitz behavior. This may be done by computing a wavelet transform of their sum and then attempting to estimate the locations and magnitudes of the extrema of the wavelet transforms of the signals using the additional a priori knowledge about their local Lipschitz properties. Several studies that are based on variations of this idea are currently being pursued by different research groups.

2.D Discrete Orthogonal Wavelet Orthogonal Transform

A second approach to eliminate the redundancy in the continuous wavelet transform consists in sampling that transform. In [17], Daubechies proposed to sample the scale parameter s on a grid $\{a^j\}_{j=-\infty}^{\infty}$. According to the discussion

in Section 3.B, the sampled transform $F(a^j, u)$ is the output of a bandpass filter centered at $a^j\overline{\omega}$ and with a root mean square bandwidth of $a^j\sigma_\omega$. Hence, we should be able to reconstruct $F(a^j, u)$ viewed as a function of u from its samples taken on the grid $\{n\beta/a^j\}_{n=-\infty}^{\infty}$ as long as β is chosen appropriately. Daubechies studied the problem of choosing α and β to obtain a non-redundant and complete representation. She showed that certain choices of (α, β) lead to a non-redundant and yet complete representation.

A valid choice for the pair (α, β) that has received considerable attention is $(\alpha, \beta) = (2, 1)$. In particular, it is shown in [17] that any square integrable signal admits the decomposition

$$f(t) = \sum_j \sum_m \sqrt{2^j} b(j; m) \psi(2^j t - m) \tag{2.D.1}$$

$$b(j; m) = \sqrt{2^j} \int_{-\infty}^{\infty} f(t) \psi(2^j t - m) dt, \tag{2.D.2}$$

where $\psi(t)$ is called a discrete orthogonal wavelet. The term "discrete" refers to the fact that (2.D.1) is a sampled version of the continuous wavelet transform. The term "orthogonal" refers to the fact that $\psi(t)$ is constructed to be orthogonal to all translates of its dilates $\psi(2^j t)$. Orthogonality of the translates and dilates of $\psi(t)$ is not necessary but may be achieved by properly constructing $\psi(t)$. The main characteristic of the discrete orthogonal wavelet transform is that it is non-redundant, i.e., any sequence $\{\sqrt{2^j} b(j; m)\}$ that is absolutely summable is a valid wavelet coefficient sequence.

2.E Construction of Discrete Orthogonal Wavelets

The wavelet $\psi(t)$ is not unique, but it is also not arbitrary. It must satisfy certain conditions that insure that the expansion in (2.D.1) holds for any square integrable function. The wavelet function, and corresponding scaling function, can be constructed to be compactly supported [17]. In the sequel, we assume that the wavelet is compactly supported.

The construction of the wavelet is based on the solution $\phi(t)$ of a two scale difference equation (a dilation equation)

$$\phi(t) = \sum_k c_k \phi(2t - k) \tag{2.E.3}$$

where $\phi(t)$ is normalized so that

$$\int \phi(t)\, dt = 1 \tag{2.E.4}$$

and $\phi(t) = 0$ outside the interval $[0, K - 1]$. This normalization implies that

$$\sum_{k=0}^{K-1} c_k = 2. \tag{2.E.5}$$

Denote by $\Phi(\omega)$ the Fourier transforms of $\phi(t)$. By taking the Fourier transform of both sides of the dilation equation (2.E.3) we obtain

$$\Phi(2\omega) = G(\omega)\Phi(\omega) \tag{2.E.6}$$

where

$$G(\omega) \triangleq \frac{1}{2}\sum_k c_k e^{-jk\omega}. \tag{2.E.7}$$

Equation (2.E.6) then implies that

$$\Phi(\omega) = \Pi_{j=1}^{\infty} G(\frac{\omega}{2^j}). \tag{2.E.8}$$

(Incidentally, it is interesting to note also that the values of $\phi(t)$ for all integers in $[0, K-1]$ may be computed by solving a simple eigenvalue problem. Specifically, it may be shown by using (2.E.3) that the vector that consists of samples of $\phi(t)$ at all integers in $[0, K-1]$ is the eigenvector of the matrix $G = [c_{2i-k}]$ corresponding to its unique largest eigenvalue which is equal to one [55]. The recursion

$$\phi(\frac{n}{2^j}) = \sum_k c_k \phi(\frac{n}{2^{j-1}} - k)$$

then determines $\phi(t)$ at all dyadic points $n/2^j$.)

The orthogonal wavelet $\psi(t)$ is constructed from $\phi(t)$ as

$$\psi(t) = \sum_k d_k \phi(2t-k) \tag{2.E.9}$$

where

$$d_k = (-1)^k c_{1-k}. \tag{2.E.10}$$

To insure that the dilates and translates of the $\psi(t)$ are orthogonal we require that

$$\sum_{k=0}^{K-1} c_k c_{k-2m} = 2\delta_{0m} \tag{2.E.11}$$

where δ_{0m} is a Kroneker delta function. This condition also insures that $\phi(2^j t - m)$ is orthogonal to $\psi(2^j t - n), j \leq m$ as long as $G(\omega)$ has no zero in the interval $[-pi/3, \pi/3]$.

Another interesting property of the wavelet decomposition that is a direct result of (2.E.9)-(2.E.11), is that (2.D.1) provides a multiresolution decomposition of $f(t)$. Specifically, it is a simple matter to show that as in the continuous wavelet transform case, the coefficients $\{b(j;m)\}$ carry information about $f(t)$

near the frequency $2^j\varpi$ and the time instant $2^{-j}m$. For fixed J, the partial sum $\sum_{j=-\infty}^{J-1}\sum_m f_{j,m}\sqrt{2^j}\psi(2^jt-m)$ provides an "approximation" to $f(t)$ up to scale 2^J. The approximation is essentially a low pass filtered version of $f(t)$ approximately bandlimited to $2^J\pi$. Furthermore, the approximation to $f(t)$ up to scale 2^J can be written in terms of translates of $\phi(2^Jt)$, i.e.

$$\sum_{j=-\infty}^{J-1}\sum_m \sqrt{2^j}f_{j,m}\psi(2^jt-m) = \sum_m a_{J,m}\sqrt{2^J}\phi(2^Jt-m) \quad (2.E.12)$$

$$a_{J,m} = \sqrt{2^J}\int_{-\infty}^{\infty} f(t)\phi(2^Jt-m)dt. \quad (2.E.13)$$

The difference between the approximations at scales 2^J and 2^{J+1} is the "detail" of the function at scale 2^J and is given by the sum $\sum_m b(J;m)\psi(2^Jt-m)$. In particular, we may rewrite (2.D.1) as

$$f(t) = \sum_{m=-\infty}^{\infty}\sqrt{2^J}a(J;m)\phi(2^Jt-m) + \sum_{j=J}^{\infty}\sum_{m=-\infty}^{\infty}\sqrt{2^j}b(j;m)\psi(2^jt-m). \quad (2.E.14)$$

An example of a wavelet which satisfies the condition (2.E.5) and (2.E.11) is given by the Haar wavelet. The Haar wavelet corresponds to the scaling function that satisfies

$$\phi(t) = \begin{cases} 1 & 0 < t < 1 \\ 0 & \text{otherwise} \end{cases}$$

The wavelet itself is then equal to

$$\psi(t) = \begin{cases} 1 & 0 < t < 1/2 \\ -1 & 1/2 \le t < 1 \\ 0 & \text{otherwise} \end{cases}.$$

Multiscale analysis using Haar wavelet exhibits good time localization but frequency localization is very poor. In other words, in the decomposition (2.D.1) the coefficients $b(j;m)$'s decay very slowly to zero. Hence the conditions (2.E.5) and (2.E.11) are not enough to construct useful wavelets because they may lead to wavelet decompositions with not enough regularity. When $f(t)$ is a generic smooth function and $\psi(t)$ has a finite support, then as n tends to infinity the integral $\int f(t)\psi(nt)\,dt$ is $O(n^{-p-1})$ if and only if the first p moments of $\psi(t)$ are zero, i.e.

$$\int_{-\infty}^{\infty} t^m\psi(t)\,dt = 0 \quad m = 0, 1, \cdots, p-1. \quad (2.E.15)$$

It may be shown that imposing the additional requirement for $\psi(t)$ to have p vanishing moments is equivalent to

$$\sum_{k=0}^{K-1}(-1)^k k^m c_k = 0 \quad m = 0, 1, \cdots, p-1. \tag{2.E.16}$$

This requirement also implies that for any smooth function $f(t)$, $\phi(t)$ and its translates approximate the function with accuracy 2^{-p}, i.e.

$$\|f(t) - \sum_k a_k \phi(2^j t - k)\| \leq \alpha 2^{-jp} \|f^{(p)}\| \text{ for suitable } a_k \tag{2.E.17}$$

where α is independent of $f(t)$. Note that this means that any polynomial of order less than p can be represented exactly using translates of $\phi(t)$ as long as (2.E.16) holds. This in turn implies that the multiresolution representation given by (2.E.14) can actually be used to decompose spaces larger than $L^2(\mathcal{R})$. In particular, any function of polynomial growth up to order $p-1$ may be represented as in (2.E.14) even though such a function is not in $L^2(\mathcal{R})$.

Condition (3.12) is an essential property of wavelet decompositions as we will see in this section which discusses applications of wavelet analysis in signal processing. Fig. 3 - Fig. 4 show examples of scaling functions and wavelet functions with various number of vanishing moments.

2.F Computing Discrete Orthogonal Wavelet Decompositions

The wavelet decomposition given by (2.E.14) can be computed recursively in scale space [37]. The procedure of [37] is based on the fact that the coefficients $\{c_k/\sqrt{2}\}$ and $\{d_k/\sqrt{2}\}$ may be viewed as the impulse responses of a pair of finite impulse response conjugate quadrature mirror filters. Note that (2.E.3) implies

$$\begin{aligned}\phi(2^j t - m) &= \sum_k \langle \phi(2^{j-1}t - m), \sqrt{2^j}\phi(2^j t - k)\rangle \sqrt{2^j}\phi(2^j t - k) \\ &= \sum_k c_{k-2m}\phi(2^j t - k).\end{aligned} \tag{2.F.1}$$

It then follows that

$$a(j-1;m) \triangleq \sqrt{2^{j-1}}\langle f(t), \phi(2^{j-1}t - m)\rangle = \frac{1}{\sqrt{2}}\sum_k c_{k-2m}a(j;k). \tag{2.F.2}$$

Similarly, using (2.E.4) we obtain

$$b(j-1;m) \triangleq \sqrt{2^{j-1}}\langle f(t), \psi(2^{j-1}t - m)\rangle = \frac{1}{\sqrt{2}}\sum_k d_{k-2m}a(j;k). \tag{2.F.3}$$

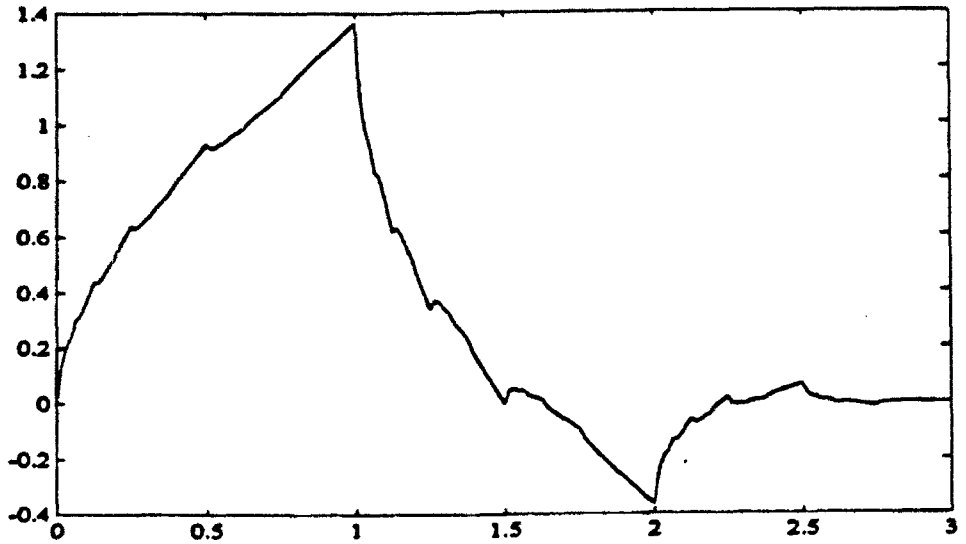

(a) Scaling function for $p = 2$

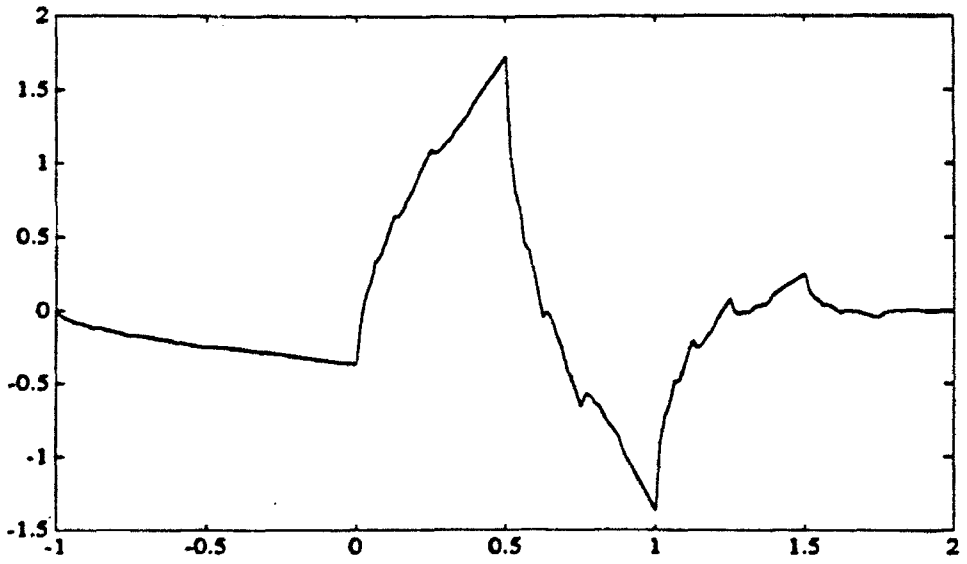

(b) Wavelet function for $p = 2$

Figure 3: Scaling function and wavelet for $p = 2$

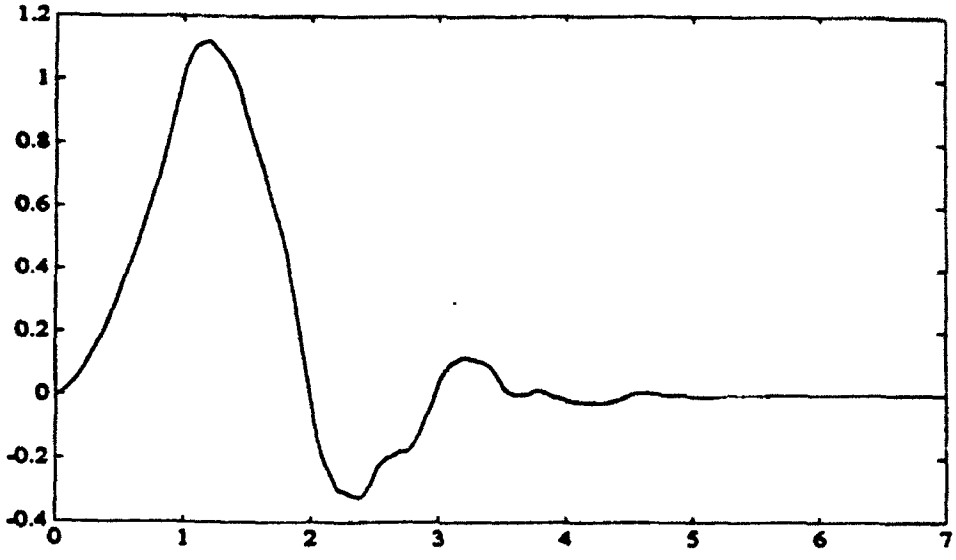

(a) Scaling function for $p = 4$

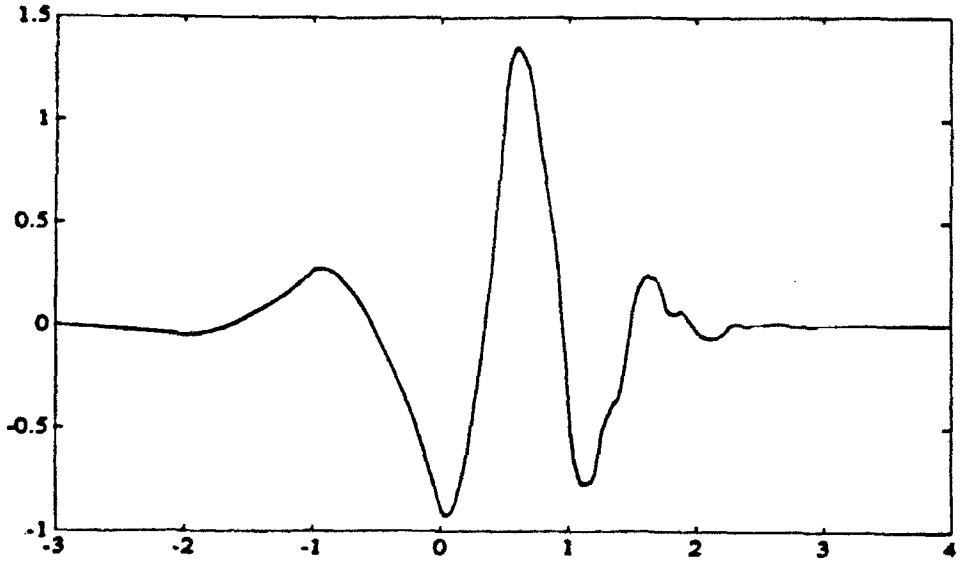

(b) Wavelet function for $p = 4$

Figure 4: Scaling function and wavelet for $p = 4$

The multiscale decomposition (2.F.2) - (2.F.3) can be implemented using filters whose impulse responses are $g(n) = c_{-n}/\sqrt{2}$ and $h(n) = d_{-n}/\sqrt{2}$ followed by decimators as in Fig. 5. In Fig. 5 $G(\omega)$ and $H(\omega)$ are the discrete Fourier transforms of $g(n)$ and $h(n)$ respectively.

Note that in practice one is given samples of a function $f(t)$ at a given scale 2^J. If J is large, those samples may be viewed as the coefficients $a(J;m)$ in an approximation $\sum_m a(J;m)\phi(2^J t - m)$ of some function $f(t)$ at scale 2^J. Then a wavelet decomposition of $f(t)$ may be computed recursively as shown in Fig. 6. Specifically, the samples of $f(t)$ are recursively low-pass and high-pass filtered with the filters $g(n)$ and $h(n)$, and the filter outputs are decimated such that only even-number coordinates are kept.

It may also be verified that the sequence $\{a(j;m)\}$ can be reconstructed from the approximation and detail sequences at the next coarser scale $\{a(j-1;m)\}$ and $\{b(j-1;m)\}$as

$$a(j;m) = \frac{1}{\sqrt{2}} \sum_k c_{m-2k} a(j-1;k) + \frac{1}{\sqrt{2}} \sum_k d_{m-2k} b(j-1;k). \qquad (2.F.4)$$

The reconstruction (2.F.4) can be implemented by upsampling and filtering with $G^*(\omega)$ and $H^*(\omega)$ as in Fig. 7.

2.G Finite Data Length Discrete Orthogonal Wavelet Transform

With a finite set of data, it is not possible to compute all $a(j;m)$'s and $b(j;m)$'s exactly, particularly those that correspond to scaled and shifted wavelets or scaling functions straddling the boundary of the interval. To handle this problem one conventionally assumes that the data is periodic outside the observation interval. Suppose we are given a finite number, $N = 2^J$, of data $\{a(J;m)\}, m = 0, \cdots, 2^J - 1$, at finest scale J. Let $\underline{a}^j$ and $\underline{b}^j$ denote $2^j \times 1$ vectors composed of 2^j point periodic approximation sequence and detail sequence at scale 2^j. Let the $2^{j-1} \times 2^j$ matrices $\mathbf{G_j}$ and $\mathbf{H_j}$ denote the matrix representation of filtering the periodized data using $g(n)$ and $h(n)$ respectively. Specifically, $\mathbf{G_j}$ and $\mathbf{H_j}$ are given by $[\mathbf{G_j}]_{ik} = c_{k-2i}/\sqrt{2}$ and $[\mathbf{H_j}]_{ik} = d_{k-2i}/\sqrt{2}$ Note that since sequences $\{c_k\}$ and $\{d_k\}$ of length $2p$ are required to produce a compactly supported wavelet with p vanishing moments [17], we are restricted to use a wavelet with p number of vanishing moments such that $2p \leq 2^j$ at scale 2^j, i.e. we have to use wavelets with a smaller number of vanishing moments at coarser scales.

It may be shown that $\mathbf{G_j}$ and $\mathbf{H_j}$ have the following properties:

$$\mathbf{G_j G_j^T} = \mathbf{H_j H_j^T} = \mathbf{I} \qquad (2.G.1)$$

$$\mathbf{G_j H_j^T} = \mathbf{H_j G_j^T} = \mathbf{0} \qquad (2.G.2)$$

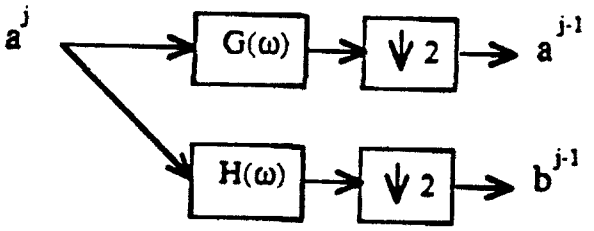

Figure 5: Analysis filter pair

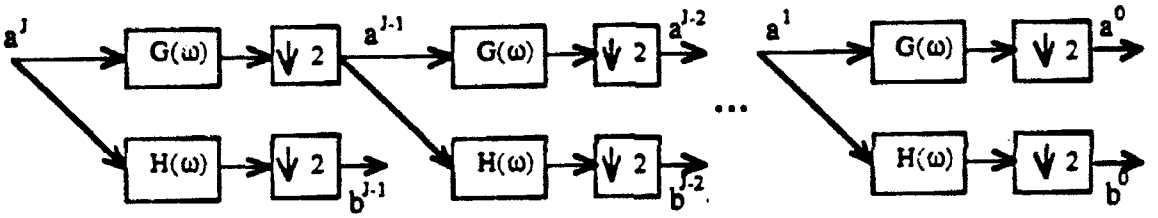

Figure 6: Discrete wavelet decomposition

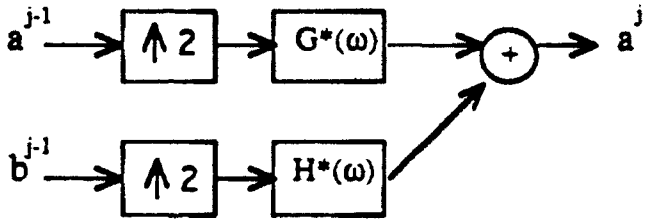

Figure 7: Synthesis filter pair

$$\mathbf{G}_j^T \mathbf{G}_j + \mathbf{H}_j^T \mathbf{H}_j = \mathbf{I} \tag{2.G.3}$$

With these filter matrices $\mathbf{G}_j$ and $\mathbf{H}_j$, the finite data multiscale decomposition may be expressed as

$$\underline{a}^{j-1} = \mathbf{G}_{j-1} \underline{a}^j \tag{2.G.4}$$

$$\underline{b}^{j-1} = \mathbf{H}_{j-1} \underline{a}^j \tag{2.G.5}$$

$$\underline{a}^j = \mathbf{G}_{j-1}^T \underline{a}^{j-1} + \mathbf{H}_{j-1}^T \underline{b}^{j-1} \tag{2.G.6}$$

where $\underline{a}^j$ and $\underline{b}^j$ are $2^j \times 1$ vectors given by

$$\begin{aligned} \underline{a}^j &= [a(j;0), a(j;1), \cdots, a(j;2^j-1)]^T \\ \underline{b}^j &= [b(j;0), b(j;1), \cdots, b(j;2^j-1)]^T. \end{aligned}$$

From (2.G.4)-(2.G.6) we have

$$\begin{aligned} \underline{a}^J &= \mathbf{G}_{J-1}^T \underline{a}^{J-1} + \mathbf{H}_{J-1}^T \underline{b}^{J-1} \\ &= \mathbf{G}_{J-1}^T \mathbf{G}_{J-2}^T \underline{a}^{J-2} + \mathbf{G}_{J-1}^T \mathbf{H}_{J-2}^T \underline{b}^{J-2} + \mathbf{H}_{J-1}^T \underline{b}^{J-1} \\ &= \mathbf{G}_{J-1}^T \mathbf{G}_{J-2}^T \cdots \mathbf{G}_0^T \underline{a}^0 + \mathbf{G}_{J-1}^T \cdots \mathbf{G}_1^T \mathbf{H}_0^T \underline{b}^0 + \mathbf{G}_{J-1}^T \cdots \mathbf{G}_2^T \mathbf{H}_1^T \underline{b}^1 \\ &\quad + \cdots + \mathbf{H}_{J-1}^T \underline{b}^{J-1}. \end{aligned} \tag{2.G.7}$$

Define

$$\mathbf{Q} = \begin{bmatrix} \mathbf{H}_{J-1}^T \\ \mathbf{H}_{J-2}^T \mathbf{G}_{J-1}^T \\ \mathbf{H}_{J-3}^T \mathbf{G}_{J-2}^T \mathbf{G}_{J-1}^T \\ \vdots \\ \mathbf{H}_0^T \mathbf{G}_1^T \mathbf{G}_2^T \cdots \mathbf{G}_{J-1}^T \\ \mathbf{H}_0^T \mathbf{G}_1^T \mathbf{G}_2^T \cdots \mathbf{G}_{J-1}^T \end{bmatrix} \tag{2.G.8}$$

and

$$\mathbf{b}^J = \begin{bmatrix} \underline{b}^{J-1} \\ \underline{b}^{J-2} \\ \vdots \\ \underline{b}^0 \\ \underline{a}^0 \end{bmatrix}. \tag{2.G.9}$$

Then

$$\underline{a}^J = \mathbf{Q}^{\mathbf{T}}\mathbf{b}^{\mathbf{J}} \tag{2.G.10}$$

and

$$\mathbf{b}^{\mathbf{J}} = \mathbf{Q}\underline{a}^J. \tag{2.G.11}$$

From (2.G.1)-(2.G.3), it is clear that $\mathbf{Q}$ is orthogonal, i.e., $\mathbf{Q}\mathbf{Q}^{\mathbf{T}} = \mathbf{Q}^{\mathbf{T}}\mathbf{Q} = \mathbf{I}$.

Equation (2.G.11) implies that wavelet transform can be computed by a multiplication of matrix $\mathbf{Q}$ and a data vector $\underline{a}^J$, hence we will call the matrix $\mathbf{Q}$ the discrete wavelet transform (DWT) matrix. The discrete wavelet transform, or multiplying a vector by matrix $\mathbf{Q}$ is more efficiently computed in the following way

$$\underline{a}^J \xrightarrow{\mathbf{P_{J-1}}} \begin{bmatrix} \underline{b}^{J-1} \\ \underline{a}^{J-1} \end{bmatrix} \xrightarrow{\mathbf{P_{J-2}}} \begin{bmatrix} \underline{b}^{J-1} \\ \underline{b}^{J-2} \\ \underline{a}^{J-2} \end{bmatrix} \xrightarrow{\mathbf{P_{J-3}}} \cdots \xrightarrow{\mathbf{P_0}} \begin{bmatrix} \underline{b}^{J-1} \\ \underline{b}^{J-2} \\ \vdots \\ \underline{b}^{0} \\ \underline{a}^{0} \end{bmatrix} = \mathbf{b}^{\mathbf{J}}$$

$$\mathbf{b}^{\mathbf{J}} = \mathbf{Q}\underline{a}^J = \mathbf{P_0}(\mathbf{P_1}(\mathbf{P_2}(\cdots(\mathbf{P_{J-1}}\underline{a}^J)\cdots) \tag{2.G.12}$$

where

$$\mathbf{P_{J-1}} = \begin{bmatrix} \mathbf{H_{J-1}} \\ \mathbf{G_{J-1}} \end{bmatrix}, \mathbf{P_{J-2}} = \begin{bmatrix} \mathbf{I_{J-2}} & 0 \\ 0 & \mathbf{H_{J-2}} \\ 0 & \mathbf{G_{J-2}} \end{bmatrix}, \mathbf{P_{J-k}} = \begin{bmatrix} \mathbf{I_{J-k}} & 0 \\ 0 & \mathbf{H_{J-k}} \\ 0 & \mathbf{G_{J-k}} \end{bmatrix}$$

where $\mathbf{I_m}$ is an $2^m \times 2^m$ identity matrix. If the analyzing wavelet has p vanishing moments, $\mathbf{H_j}$ and $\mathbf{G_j}$ have $2p$ number of nonzero elements per row. Hence the number of multiplications for computing discrete wavelet transform is approximately $4pN$ where $N = 2^J$. Note that the number of operations for computing DWT is proportional to N whereas computation of FFT requires $N \log_2 N$ operations.

2.H Generalization of Wavelet Decompositions

The connection between wavelet decompositions and 2 band perfect reconstruction filter banks was briefly discussed in the above subsection. Since it is possible to construct M-band perfect reconstruction filter banks, it is natural to ask whether an M-band generalization of the wavelet decomposition (2.D.1) exists. It turns out that the answer to this question is affirmative. In particular, it is shown in [74] (see also [69]) that any square integrable signal $f(t)$

may be expanded in terms of a scaling function $\phi(t)$ and $M-1$ M-band wavelet functions as

$$f(t) = \sum_{m=-\infty}^{\infty} \sqrt{M^J} a(J;m)\phi(2^J t - m) + \sum_{n=1}^{M-1} \sum_{j=J}^{\infty} \sum_{m=-\infty}^{\infty} \sqrt{M^j} b(j;m)\psi_n(M^j t - m). \tag{2.H.1}$$

The scaling function $\phi(t)$ obeys a two scale difference equation of the form

$$\phi(x) = \sum_k c_k \phi(Mx - k) \tag{2.H.2}$$

while the wavelet functions $\psi_n(x)$ are given by

$$\psi_n(x) = \sum_k d_{n,k}\phi(Mx - k), \quad n = 1, 2, \cdots, M-1. \tag{2.H.3}$$

As in the 2-band case, the $M-1$ wavelets $\psi_n(t)$ are characterized by the fact that they have p vanishing moments, with $p > 1$, i.e.

$$\int_{-\infty}^{\infty} t^m \psi_n(t)\, dt = 0 \quad m = 0, 1, \cdots, p-1. \tag{2.H.4}$$

Furthermore, all translates and dilates of the $M-1$ wavelets $\psi_n(t)$ are mutually orthogonal. Finally, we also have

$$\sum_{n=1}^{M-1} \sum_{j=-\infty}^{J-1} \sum_{m=-\infty}^{\infty} \sqrt{M^j} b(j;m)\psi_n(M^j t - m) = \sum_{m=-\infty}^{\infty} \sqrt{M^J} a(J;m)\phi(2^J t - m). \tag{2.H.5}$$

i.e. the M-band wavelet decomposition also induces a multiresolution decomposition of $L^2(\mathcal{R})$. A complete characterization of the coefficients $\{c_k\}$ and $\{d_{n,k}\}$ that lead to valid wavelets is given in [74]. The advantages of M-band wavelet decompositions over the 2-band case are the additional degrees of freedom available to the designer in choosing the sets $\{c_k\}$ and $\{d_{n,k}\}$ and the more compact signal representations that generally result from the use of such decompositions.

Wavelet decompositions have also be extended to the M-dimensional case. The simplest extension is mentioned in [37] and uses scaling functions and wavelets that are equal to simple products of 1-D scaling and wavelet functions. More flexible non- separable wavelets are discussed in [13], [33] and [67].

3 MAIN RESULTS

The main objective of this research was to explore the role of wavelet theory in signal and information representation and extraction. More specifically, during the period February 1992 to January 1993 we studied two information extraction problems: separating plane waves radiated or reflected by a target from a background noise process with an unknown correlation structure and estimating a distributed range-Doppler target reflectivity map to within an error of a given energy using a minimal number of radar probing waveforms.

Our goal in studying the first problem was to show that it is possible to exploit differences in the structures of the correlations of the wavelet transforms of the response of an array of sensors to plane waves and its response to wide classes of correlated background noises. We succeeded in establishing this fact and constructed an iterative method for estimating the directions of arrival of plane waves mixed a background noise process with an unknown correlation structure.

In the second problem, our aim was to investigate the role of wavelets in radar imaging. Wavelets seemed to have a natural role in radar imaging. A wavelet representation provides a decomposition of a signal in terms of translates and dilates of a single waveform. On the other hand, the reflection process in radar imaging induces a translation and dilation of the transmitted waveform. Our work showed that the optimal set of waveforms that must be transmitted to obtain the best estimate of any range-Doppler target reflectivity function is a set of N wavelet waveforms that are derived from the target reflectivity function itself.

We also investigated two signal representation problems. The first problem was more theoretical in nature and involved constructing a simple test for the completeness of an arbitrarily sampled redundant dyadic wavelet transform as well as a direct computationally efficient method for reconstructing a signal from a complete arbitrary sampling of its dyadic wavelet transform. The second problem was a transparent audio coding problem. The objectives there were to establish that the regularity of wavelets is important in coding applications and that dynamic adaptation of wavelets to the underlying signal can lead to substantial reductions in bit rate. Another goal was to study the general problem of adaptively choosing an analysis discrete orthogonal wavelet to minimize a cost function (e.g., bit rate in this application) subject to satisfying a given constraint (e.g., quality of the encoded signal in this application).

In what follows we briefly summarize the results that we have obtained in the period February 1992-January 1993. A more complete description of these results can be found in several papers that will appear or have been submitted for publication in the *IEEE Transactions on Signal Processing* and the *IEEE Transactions on Image Processing* [53], [58], [59], [76]. Re-prints or pre- prints of these papers are available from the principal investigator and from AFOSR. Summaries of these papers have also been published in the proceedings of two

conferences and a workshop [52], [57], [62], [75].

We continue to perform research in the aboveareas and on two related problems (adaptive beamforming and integrated target sensing and recognition) with AFOSR support.

3.A Wavelet Domain Array Processing

Most modern high resolution bearing estimation techniques assume that the background noise process has a known covariance function. These techniques tend to perform poorly in situations where the covariance structure of the noise is unknown. To address these situations, several approaches have been proposed in recent years, e.g., [34], [47], [45], [56], [70].Some of these techniques assume a particular model for the noise process, e.g., an auto-regressive-moving-average (ARMA) model. Others eliminate the effect of the unknown noise covariance by assuming a least informative prior distribution for the noise covariance function. In our work we derived an alternative approach. This approach requires only that the spatial correlation function of the noise process decays asymptotically to zero as the distance between samples of the noise tends to infinity.

For simplicity of exposition, we will assume here that the noise process and a set of narrow band plane waves are sampled by a uniform linear array. Note however, that the ideas described here can be applied as well to non-linear and non-uniform arrays as well as to wide-band signals.

We shall denote by $f(n)$ the output of the n^{th} sensor in the array. Recall that in an M-band wavelet decomposition a signal $x(n)$ is decomposed using a regular cascade of perfect reconstruction filter banks (c.f. Fig. 8). Each bank consists of M filters $H_k(z)$, $k = 0, 1, \cdots, M-1$. We will assume here that the filters $H_k(z)$, $k = 1, \cdots, M-1$ have p zeros at $z = 1$. (Recall that each of these filters must have at least one zero at $z = 1$.) Note that by using the "Noble identities" of Section 2.B in [64] it follows that Fig. 8.a may be redrawn as in Fig. 8.b. Following wavelet terminology, we shall call each of the signals $x_k(n)$ in Fig. 8.b the "multiresolution" component or the "detail" of $x(n)$ in band k. We also introduce a partial ordering of the outputs $x_k(n)$ by numbering the analysis stages from left to right. We use the notation $\rho(k)$ to denote the order of the analysis stage in which $x_k(n)$ is computed. We shall then say that $x_k(n)$ is a "higher resolution" component of $x(n)$ than $x_{k'}(n)$ if $\rho(k) < \rho(k')$.

Since the filters $H_k(z)$, $k = 1, \cdots, M-1$, in Fig. 8 have at least p zeros at $z = 1$, the filters $W_k(z)$ that produce the details of $f(n)$ will also have at least p zeros at $z = 1$. Hence, if we use $w_k(n)$ to denote the impulse response of the filters $W_k(z)$, we note that

$$\sum_m m^n w_k(m) = 0 \qquad n = 0, 1, \cdots, p-1 \qquad (3.A.1)$$

We shall see in the next section that (3.A.1) will play a key role in obtaining sparse representations for a large class of covariance matrices.

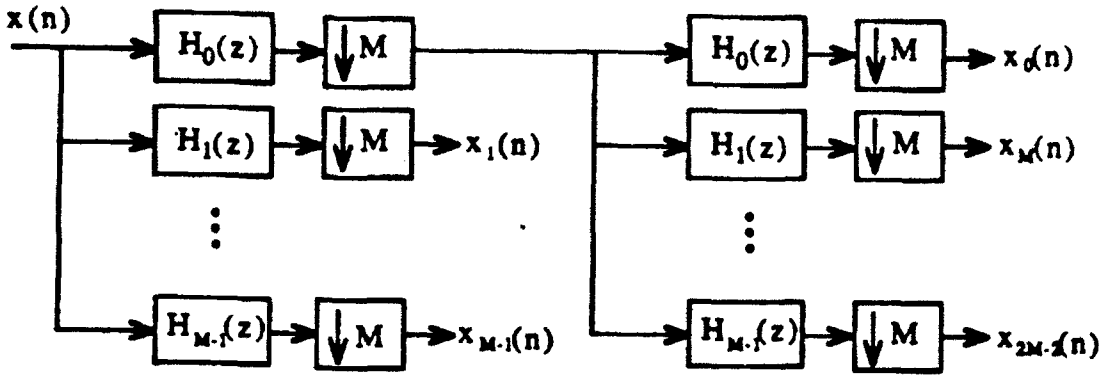

(a)

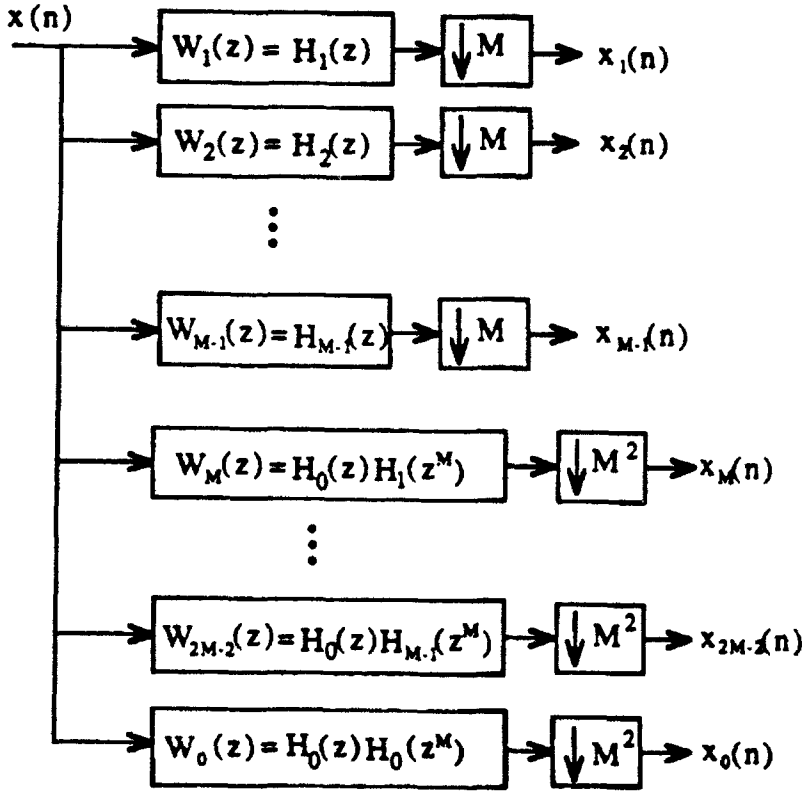

(b)

Figure 8: A Two Stage M-band Decomposition

3.A.1 Asymptotic Form of the Correlation Function of the Wavelet Transform Coefficients of the Outputs of a Linear Uniform Array

First, observe that the covariance $R(m,n)$ of $f(n)$ is a sampled version of a continuous 2-D function $R(t,s)$. Denote by $R_w^{j,k}(m,n) = E[f_j(m)f_k(n)]$ the cross- covariance between the m^{th} component of $f(n)$ in the j^{th} band and the n^{th} component of $f(n)$ in the k^{th} band. Observe that using the notation that we introduced above we may express $R_w^{j,k}(m,n)$ as

$$R_w^{j,k}(m,n) = \sum_{m' \in \mathcal{S}_j} \sum_{n' \in \mathcal{S}_k} R(M^{\rho(j)}m - m', M^{\rho(k)}n - n')w_j(m')w_k(n'). \tag{3.A.2}$$

In (3.A.2) $\mathcal{S}_k$ is the support of the filter $w_k(n)$, i.e., the set of indices n for which $|w_k(n)| \neq 0$. Our objective is to study the asymptotic behavior of $R_w^{j,k}(m,n)$ as $\max(m,n)$ tends to infinity while $\min(m,n)$ is finite and fixed. Without loss of generality we will assume here that $n = \min(m,n)$ and is fixed while $m = \max(m,n)$.

Assume now that all the partial derivatives $\partial^{l+k}R(t,s)/\partial t^k \partial s^l$ of $R(t,s)$ exist for $0 \leq l,k \leq 2p$. Following a technique introduced in [42] to study wavelet decompositions of operators and also used in [6], we first use Taylor's theorem of the mean for smooth 2-D functions to write

$$\begin{aligned}
&R(M^{\rho(j)}m - m', M^{\rho(k)}n - n') \\
&= R(M^{\rho(j)}m, M^{\rho(k)}n) + \sum_{i=1}^{2p-1} \frac{1}{i!} \left[(-m')\frac{\partial}{\partial t} + (-n')\frac{\partial}{\partial s}\right]^i R(t,s) \Bigg|_{\substack{t = M^{\rho(j)}m \\ s = M^{\rho(k)}n}} \\
&+ \frac{1}{(2p)!} \left[(-m')\frac{\partial}{\partial t} + (-n')\frac{\partial}{\partial s}\right]^{2p} R(t,s) \Bigg|_{\substack{t = M^{\rho(j)}m - \theta m' \\ s = M^{\rho(k)}n - \theta n'}} \quad \text{for some } 0 \leq \theta \leq 1 \\
&= R(M^{\rho(j)}m, M^{\rho(k)}n) + \sum_{i=1}^{2p-1} \frac{1}{i!} \sum_{l=0}^{i} \binom{i}{l} (-m')^l (-n')^{i-l} \frac{\partial^i R(t,s)}{\partial t^l \partial s^{i-l}} \Bigg|_{\substack{t = M^{\rho(j)}m \\ s = M^{\rho(k)}n}} \\
&+ \frac{1}{(2p)!} \sum_{l=0}^{2p} \binom{2p}{l} (m')^l (n')^{2p-l} \frac{\partial^{2p} R(t,s)}{\partial t^l \partial s^{2p-l}} \Bigg|_{\substack{t = M^{\rho(j)}m - \theta m' \\ s = M^{\rho(k)}n - \theta n'}} \\
&\quad \text{for some } 0 \leq \theta \leq 1.
\end{aligned} \tag{3.A.3}$$

If we substitute this expression into (3.A.2) and use the fact that the first p moments of $u_j(n)$ and $w_k(n)$ are zero we obtain

$$|R_w^{j,k}(m,n)| \leq \frac{1}{(2p)!} \sum_{l=0}^{2p} \binom{2p}{l} \sum_{m' \in \mathcal{S}_j} \sum_{n' \in \mathcal{S}_k}$$

$$\sup_{\substack{(m',n')\in S_j\times S_k\\ \theta\in[0,1]}} \left|\frac{\partial^{2p}R(t,s)}{\partial t^l \partial s^{2p-l}}\right|_{\substack{t=M^{\rho(j)}m-\theta m'\\ s=M^{\rho(k)}n-\theta n'}} |(m')^l (n')^{2p-l} w_j(m') w_k(n')|$$

$$\leq C \sup_{\substack{(m',n')\in S_j\times S_k\\ \theta\in[0,1]\\ l\in\{0,1,\cdots 2p\}}} \left|\frac{\partial^{2p}R(t,s)}{\partial t^l \partial s^{2p-l}}\right|_{\substack{t=M^{\rho(j)}m-\theta m'\\ s=M^{\rho(k)}n-\theta n'.}} \qquad (3.A.4)$$

In the above equation C is a finite constant given by

$$C=\frac{1}{(2p)!}\sum_{l=0}^{2p}\binom{2p}{l}\sum_{m'\in S_j}|(m')^l w_j(m')|\sum_{n'\in S_k}|(n')^{2p-l}w_k(n')|. \qquad (3.A.5)$$

Hence, as long as all terms $|\frac{\partial^{2p}R(m,n)}{\partial m^l \partial n^{2p-l}}|$, $0\leq l\leq 2p$, decay faster to zero than $|R(m,n)|$ itself as m tends to infinity (i.e. as long as $\lim_{m\to\infty}(|\frac{\partial^{2p}R(t,s)}{\partial t^l \partial s^{2p-l}}|)/|R(m,n)|=0, \forall l\leq 2p$), $R_w^{j,k}(m,n)$ will decay faster than $R(m,n)$ as m tends to infinity. In particular, the multiresolution components of $x(n)$ will effectively be partially uncorrelated.

Consider now the case where $R(m,n)$ behaves asymptotically as

$$R(m,n)=m^{\alpha(n)}e^{-\beta(n)m}(a_0(n)+o(1))+a_1(n) \qquad \text{as } m\to\infty. \qquad (3.A.6)$$

In the above equation the function $\beta(n)$ may have both a real and an imaginary part. However, its real part is assumed to be a non-negative and non-decreasing function of n. Its imaginary part must be zero if its real part is zero. The function $\alpha(n)$ is only assumed to be a non-increasing function of n. The class of processes with covariance functions that behave asymptotically as (3.A.6) is quite large. For example it includes all stationary processes that can be obtained by passing white noise through a rational filter. The covariance functions of such processes decay exponentially fast to zero for fixed n as m tends to infinity. It also includes nonstationary process such as a sampled version of a fractional Brownian motion [41]- [2] whose covariance function is given by

$$R(m,n)=\frac{V_H}{2}(|m|^{2H}+|n|^{2H}-|m-n|^{2H}), \quad 0<H<1.$$

For fixed n, this covariance function behaves asymptotically as (3.A.6) with $\beta(n)=0$. The fractionally differenced white noise process [26]-[20] and samples of the underwater background acoustic noise in shallow water taken along any straight line [8] are other examples of nonstationary processes with covariance functions that behave asymptotically as (3.A.6).

As m tends to infinity and since the sums in (3.A.2) are finite, we may rewrite (3.A.2) as

$$R_w^{j,k}(m,n) = \sum_{n'\in S_k} w_k(n')\{\sum_{m'\in S_j} w_j(m')$$

$$[(M^{\rho(j)}m - m')^{\alpha(M^{\rho(k)}n-n')}e^{-\beta(M^{\rho(k)}n-n')(M^{\rho(j)}m-m')}$$
$$(a_0(M^{\rho(k)}n - n') + o(1)) + a_1(M^{\rho(k)}n - n')]\} \tag{3.A.7}$$

where we have used (3.A.6). Recalling that $\Re(\beta(\cdot)) \geq 0$, define the quantities $\alpha_0(M^{\rho(k)}n)$ and $\beta_0(M^{\rho(k)}n)$ as

$$\beta_0(M^{\rho(k)}n) = \beta(M^{\rho(k)}n - n_0) \tag{3.A.8}$$
$$n_0 \in \aleph_\beta = \{n' \in \mathcal{S}_k : \Re(\beta(M^{\rho(k)}n - n') = \inf_{n' \in \mathcal{S}_k} \Re(\beta(M^{\rho(k)}n - n')\} \tag{3.A.9}$$
$$\alpha_0(M^{\rho(k)}n) = \sup_{n' \in \aleph_\beta} \alpha(M^{\rho(k)}n - n'). \tag{3.A.10}$$

When $\Re(\beta_0(M^{\rho(k)}n) \neq 0$ it may be readily verified that

$$\lim_{M^{\rho(j)}m \to \infty} \frac{|R_w^{j,k}(m,n)|}{[(M^{\rho(j)}m)^{\alpha_0(M^{\rho(k)}n)}e^{-\Re(\beta_0(M^{\rho(k)}n))(M^{\rho(j)}m))}]} = c_0(M^{\rho(k)}n), \tag{3.A.11}$$

where

$$c_0(M^{\rho(k)}n) = |\sum_{n' \in \aleph_\alpha} \sum_{m' \in \mathcal{S}_j} w_k(n')w_j(m')e^{\beta(M^{\rho(k)}n-n')m'}a_0(M^{\rho(k)}n - n')| \tag{3.A.12}$$
$$\aleph_\alpha = \{n' \in \aleph_\beta : \alpha(M^{\rho(k)}n - n') = \sup_{n' \in \aleph_\beta} \alpha(M^{\rho(k)}n - n')\} \tag{3.A.13}$$

This of course implies that $|R_w^{j,k}(m,n)|$ decays asymptotically as $(M^{\rho(j)}m)^{\alpha_0(M^{\rho(k)}n)}$ $e^{-\Re(\beta_0(M^{\rho(k)}n)M^{\rho(j)}m)}$. Since $\beta(\cdot)$ and $\alpha(\cdot)$ are non- decreasing and non-increasing functions of their arguments respectively, this also means that $|R_w^{j,k}(m,n)|$ decays asymptotically to zero at a rate much faster than $R(m,n)$.

On the other hand, when $\beta(n) = 0$ identically in (3.A.6), it may be verified using (3.A.1) that

$$\lim_{M^{\rho(j)}m \to \infty} \frac{|R_w^{j,k}(m,n)|}{(M^{\rho(j)}m)^{\alpha_0(M^{\rho(k)}n)-p}} = c_1(M^{\rho(k)}n), \tag{3.A.14}$$

where

$$\alpha_0(M^{\rho(k)}n) = \sup_{n' \in \mathcal{S}_k} \alpha(M^{\rho(k)}n - n') \tag{3.A.15}$$
$$c_1(M^{\rho(k)}n) = \frac{\alpha_0(\alpha_0 - 1)\cdots(\alpha_0 - p + 1)}{p!} \sum_{n' \in \mathcal{S}_k} w_k(n') \sum_{m' \in \mathcal{S}_j} w_j(m')$$
$$|m'|^p \left(1 + \left|\frac{m'}{M^{\rho(j)}m}\right|\right)^{\alpha_0 - p} \left|a_0(M^{\rho(k)}n - n')\right|. \tag{3.A.16}$$

Note that in this case as m tends to infinity, $R(m,n)$ may either decrease hyperbolically (instead of exponentially) fast to a constant which may be a function of n. It may also increase without bound. However, according to (3.A.14) $R_w^{j,k}(m,n)$ decreases to zero asymptotically as $m^{\alpha_0(M^{s(k)}n)-p}$ as long as $\alpha_0(\cdot) < p$. In particular, $R_w^{j,k}(m,n)$ decreases once more to zero asymptotically at a rate much faster than $R(m,n)$.

Finally, observe that if $R(m,n)$ consists of oscillatory components, both $\alpha(n)$ and $\beta(n)$ in (3.A.6) will be zero. In this case, the wavelet transform does not decorrelate the process.

The observations that we have made here are illustrated in Figs. 9.a and 9.b. Fig. 9.a shows the magnitude of the entries of the correlation matrices of the 8-band wavelet coefficients corresponding to five uncorrelated sources of powers -17 dB, -2.8 dB, -23 dB, -6.38 dB and -6.38 dB (relative to the total noise power) impinging respectively at $45°, 70°, 75°, 85°$ and $90°$ on a 64 elements uniform linear array with inter-sensor separation of $\lambda/2$. On the other hand Fig. 9.b shows the magnitude of the entries of the correlation matrices of the 8-band wavelet coefficients of a 2 pole AR background noise process. The poles of the process were at $0.96e^{-j1.1107}$ and $0.7e^{j\pi/2}$. Their respective powers were -27 dB and -0.0087 dB relative to the total noise power. This noise process was constructed by Dr. N. Owsley from NUSC. It is a good model for the background noise observed in the ocean in a particular set of experiments. Observe that the correlation matrix of the wavelet transform of the signal part consists of plateaus while that of the noise consists of line structures .

3.A.2 Wavelet Domain Bearing Estimation in the Presence of Correlated Noise of Unknown Structure

The bearing estimation approach that we proposed is based on the results that we described in Section 1.A.1. It consists in computing an estimate of the correlation matrix of the M-band wavelet coefficients corresponding to the noiseless sensor outputs. The procedure begins by estimating the correlation matrix of the M-band wavelet coefficients corresponding to the noisy sensor outputs using an average of the outer products of vectors of the M-band wavelet coefficients corresponding to several snapshots of the sensor outputs. Next, we zero the entries of the estimated correlation matrix that lie along any observed linear structure. These linear patterns can be parts of diagonals or slanted diagonals. They are easily detected using image processing techniques. The above step essentially cancels the contribution of the noise correlation matrix to the computed wavelet domain correlation matrix.

Denote by $\mathbf{R}_s$ the autocorrelation matrix corresponding to the wavelet coefficients of the autocorrelation of the plane waves. One is then left with a perturbed version of the matrix $\mathbf{R}_s$ with missing entries. The perturbation is a function of the number of snapshots used, the signal-to-noise ratio (i.e. the accuracy with which the correlation matrix of the M-band wavelet coefficients

corresponding to the sensor outputs is estimated) and the degree to which the M-band wavelet decomposition decorrelates non-time-synchronous wavelet coefficients of the noise process. By computing the eigenvectors corresponding to a set of smallest eigenvalues of the matrix $\mathbf{R}_s$ with missing elements and by using the inverse wavelet transform of the corresponding eigenvectors in an eigenstructure based technique (e.g. MUSIC, ROOT MUSIC, etc. [1]), one is then able to compute a preliminary estimate of the frequencies of the line spectrum or the directions of arrivals of the plane waves. Note that at this stage it may not be possible to resolve all sources. Using those estimates, one then computes estimates of the entries of $\mathbf{R}_s$ which had been zeroed. These estimates are then used to fill the zeroed entries of the estimated wavelet correlation matrix and the procedure is repeated on the resulting matrix. The whole process is repeated until convergence. A flow chart of the procedure is given in Fig. 10.

The procedure implicitly solves a non-linear least squares fitting problem. It can be shown that it is guaranteed to converge to a local minimum. It is initialized with a guess obtained using any of the traditional approaches together with any other information that may be obtained by looking at the structures of the plateaus in the correlation matrix of the wavelet domain data. Experience has shown that such an initialization leads to good results. The procedure was compared to more traditional approaches in a number of scenarios including the one described at the end of Section 1.A.1. In that scenario, none of the traditional approaches was able to detect the sources at 45° and 75° even when exact correlation matrices are used. On the other hand, the proposed approach was able to detect all sources when exact covariances were used or when more than 20 snapshots were assumed to be available. Fig. 11 shows the results obtained in another scenario using a simpler version of the proposed procedure in which positions of the entries which are zeroed is prefixed to be the main diagonal and some slanted diagonals regardless of where the linear structures appear. The exact source location are marked with tics on the plots. Each simulation (one curve on the attached plot) assumes that 100 data snapshots are available for processing. Note that MUSIC detects one source and is unable to resolve two others. The simplified version of our procedure is able to resolve these two sources but cannot detect the other two weak sources. The full technique is needed to detect these latter two sources.

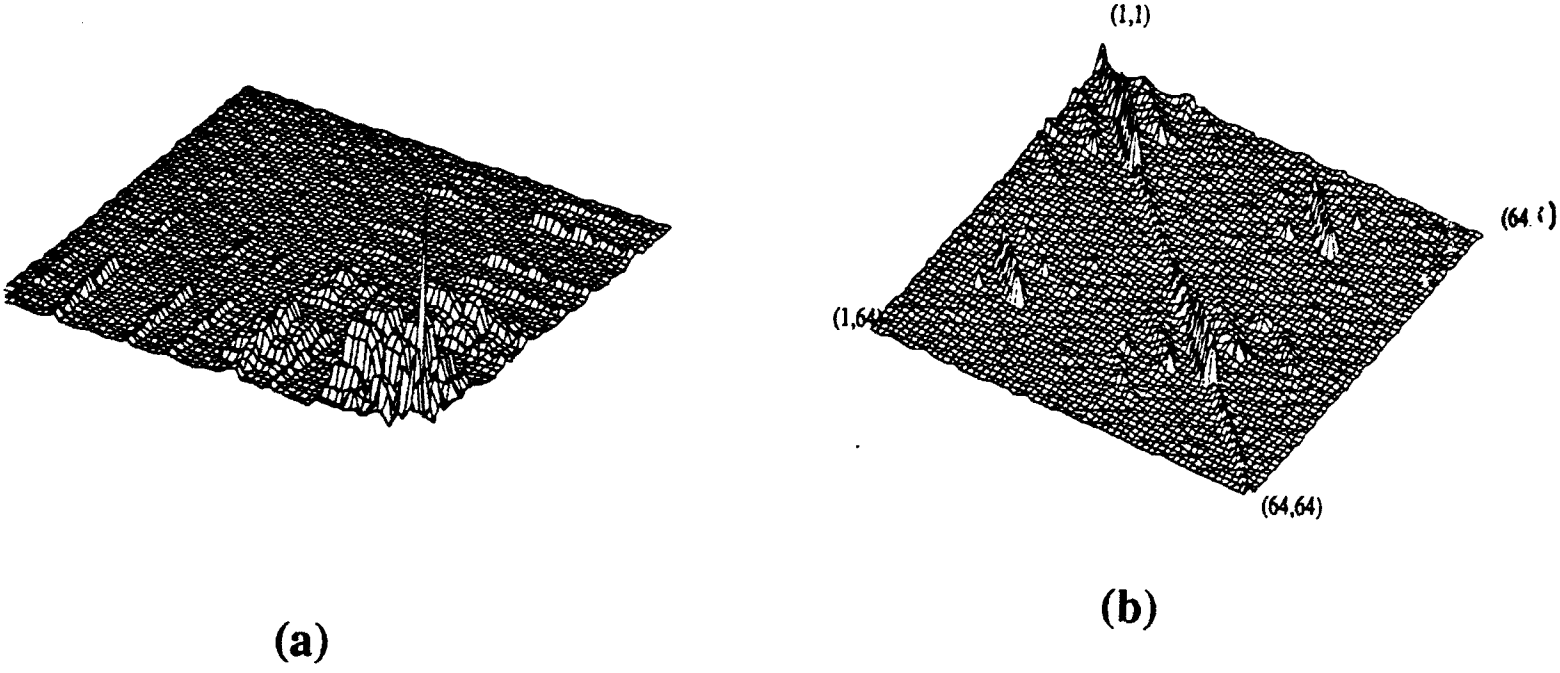

Figure 9: Magnitude of the Entries of the Correlation Matrix of the Wavelet Coefficients Corresponding to : (a) The five sources at45°, 70°, 75°, 85° and 90° (b) BackgroundNoise.

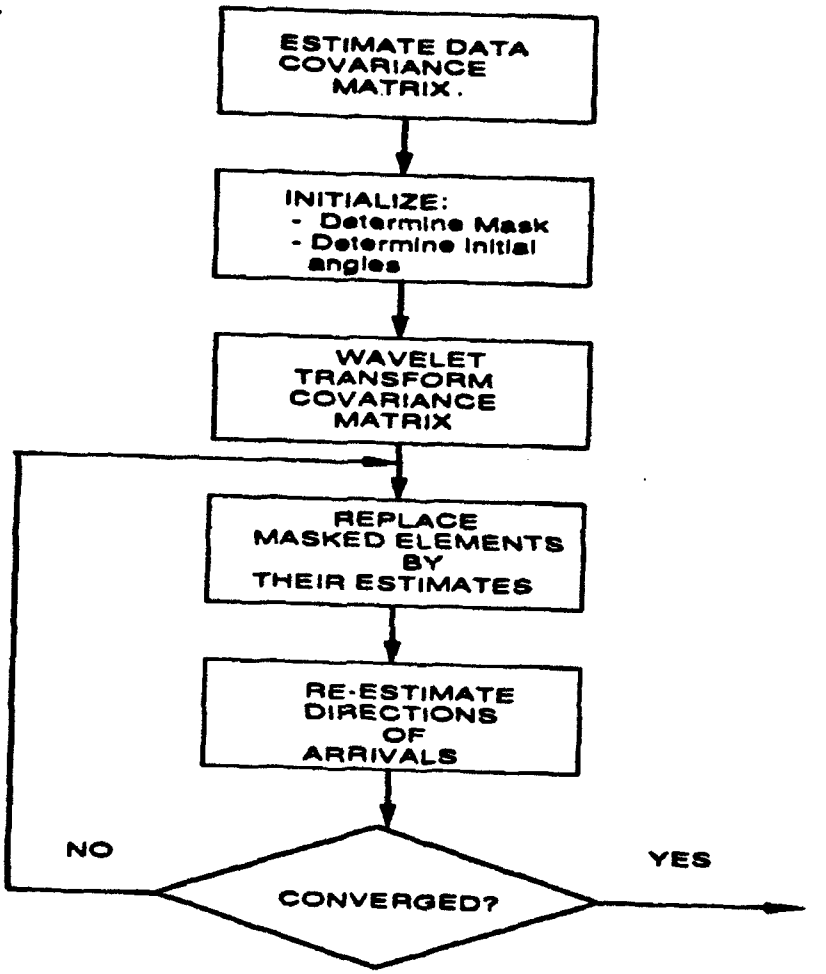

Figure 10: Flow Chart Description Of The Proposed Bearing Estimation Approach

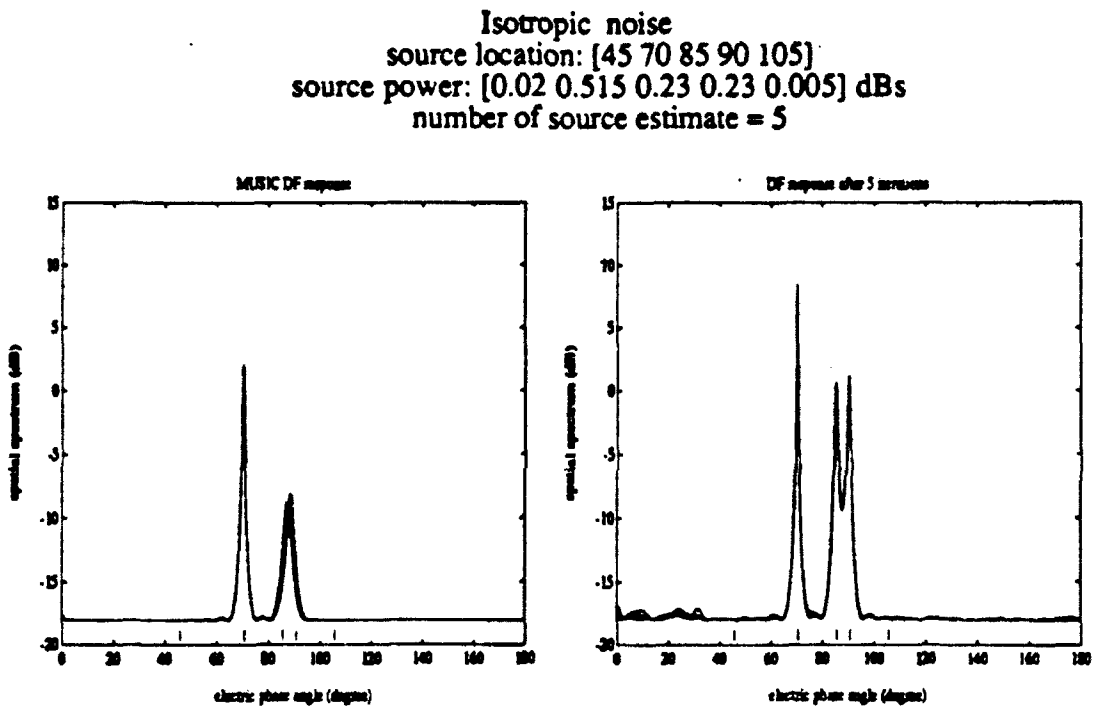

Figure 11: Performance Of MUSIC And A Simplified Version Of The Proposed Technique In A Given Scenario.

3.B Optimal Radar Range-Doppler Imaging

The main contribution of our work in the area of radar imaging was to show that the most accurate reconstruction of a range-Doppler target density that can be obtained using only N waveforms and their echoes results from transmitting the singular functions corresponding to the N largest singular values of two kernels derived from the target density. These singular functions are valid wavelets that obey an additional orthogonality constraint in the frequency domain. We have used this result to develop a solution to the problem of choosing a set of N waveforms to reconstruct with high accuracy an arbitrary unknown target range-Doppler density function.

Note that in practice the important question is how to construct the most accurate approximation to the range-Doppler target density by illuminating the target for a maximum of T seconds. This problem is related to the one that is addressed here since the N waveforms will have a total duration equal to the sum of their individual durations plus the duration of all silence intervals separating the waveforms. The length of these silence intervals is determined from a coarse a priori knowledge about the support of $D(x, y)$. If the radar selects the transmitted waveforms from a fixed library based on the approach presented here, the individual durations would be known a priori. Since the theory developed in our work also identifies the relative importance of each transmitted waveform in the reconstruction, it is possible to use T to select an appropriate subset of N individual waveforms for optimal imaging of the target in less than T seconds.

3.B.1 Problem Formulation

Consider first a point reflector at a distance $r(t_0)$ from a monostatic radar at time t_0. Let s(t) be the waveform transmitted by the radar. We will assume here that the echo received by the radar at time t is given by

$$As(t - \tau(t)) \tag{3.B.1}$$

where A is a constant determined by the reflection properties of the point target and the propagation characteristics of the medium and $\tau(t)$ is the total delay incurred by the part of the waveform that arrives at the radar at time t. Note that

$$\tau(t) = \frac{2}{c} r(t - \frac{1}{2}\tau(t)) \tag{3.B.2}$$

where c is the velocity of propagation of the electromagnetic waves in the medium.

It is convenient to express $\tau(t)$ as a power series over the signal duration. In particular, if the change in the velocity of the reflector over the illumination

time (duration of $s(t)$) is negligible compared to c, then we find that [32]

$$\tau(t) \approx x + \frac{2v(x/2)}{c + v(x/2)}(t - x) \tag{3.B.3}$$

where x is an arbitrary reference time instant and $v(x/2)$ is the velocity of the point reflector at time $x/2$ along the line of sight. Note that it follows from (3.B.2) that the range of the target at time $t = x/2$ is $cx/2$. Hence, the received waveform at time t will have the form $Af(y(t-x))$ where $y = (c - v(x/2))/(c + v(x/2))$. This is the exact broadband form of the echo rather than the usual narrow band approximation used in the literature. This formulation of the echo takes care of range-migration effects automatically.

Suppose now that the target consists of a continuum of point reflectors located at various ranges, moving with different velocities with respect to the radar and having different reflectivities. Assuming that reflection and propagation are linear and that all parts of the target are illuminated equally, the echo $e(t)$ due to the target will have the form

$$e(t) = \int_0^\infty dy \int_{-\infty}^\infty dx\, D(x,y)s(y(t-x)). \tag{3.B.4}$$

In the above equation $D(x,y)$ is the reflectivity of a point target located at range $cx/2$ and moving with velocity $(1-y)c/(1+y)$ at time $x/2$. Since a negative range is meaningless, $D(x,y) = 0$ for all $x < 0$. Our goal in the next section will be to reconstruct the best approximation to $D(x,y)$ by recording the echoes due to a fixed number N of transmitted waveforms.

3.B.2 Approximation of a known a $D(x,y)$ using a set of waveforms and echoes

First observe that (3.B.4) has the same form as an inverse wavelet transform. Specifically, if $\psi(t)$ is a valid wavelet function then any square integrable signal $f(t)$ can be written as

$$f(t) = \frac{1}{C_\psi} \int_0^\infty dy \int_{-\infty}^\infty dx\, F(x,y)\sqrt{y}\psi(y(t-x)) \tag{3.B.5}$$

where C_ψ is a constant that depends on $\psi(t)$ and $F(x,y)$ is the continuous wavelet transform of $f(t)$ with respect to $\psi(t)$. This observation seems to suggest then that one can reconstruct $D(x,y)$ by transmitting a single valid wavelet function $\psi(t)$ and computing the wavelet transform of the echo. Unfortunately, as observed in [44] and [36], following such an approach simply yields the projection of $D(x,y)$ onto the range of the wavelet transform with respect to $\psi(t)$.

Clearly the problem that we are addressing involves reconstructing a 2-D function from 1-D observations. Thus, in general, reconstructing an arbitrary

$D(x,y)$ will require transmitting and recording an infinite number of waveforms and echoes. Suppose on the other hand that we are restricted to using N or less waveforms. How can we optimize the choice of these waveforms to get the most accurate approximation of $D(x,y)$ in the norm $||D(x,y)||^2 = \int_0^\infty dy \int_{-\infty}^\infty dx|D(x,y)|^2$? We will answer this question by first assuming that $D(x,y)$ is actually known. The answer that we obtain will then guide our choice of transmitted waveforms for the actual case where $D(x,y)$ is unknown.

By taking the Fourier transform of (3.B.4) we obtain

$$E(\omega) = \int_0^\infty \Delta(\omega, y)\frac{S(\frac{\omega}{y})}{y}. \tag{3.B.6}$$

In the above equation $\Delta(\omega,y)$ is the Fourier transform of $D(x,y)$ with respect to x, i.e.

$$\Delta(\omega,y) = \int_{-\infty}^\infty D(x,y)e^{-j\omega x}dx. \tag{3.B.7}$$

Define $E_+(\omega) = E(\omega)$ for $\omega \geq 0$ and $E_+(\omega) = 0$ otherwise. Similarly, let $E_-(\omega) = E(\omega)$ for $\omega < 0$ and $E_-(\omega) = 0$ otherwise. Now let us change the variable of integration by defining $u = \omega/y$. With this change of variable of integration (3.B.6) yields the following two integrals

$$E_+(\omega) = \int_0^\infty T_+(\omega,u)S(u)\frac{du}{u} \tag{3.B.8}$$

and

$$E_-(\omega) = \int_{-\infty}^0 T_-(\omega,u)S(u)\frac{du}{|u|}. \tag{3.B.9}$$

In the above equations $T_+(\omega,u) = T(\omega,u)$ for $\omega \geq 0$ and $T_+(\omega,u) = 0$ otherwise, $T_-(\omega,u) = T(\omega,u)$ for $\omega < 0$ and $T_+(\omega,u) = 0$ otherwise and $T(\omega,u) = \Delta(\omega,\omega/u)$. Note that $T_\pm(\cdot,\cdot)$ are kernels of two maps that take $L^2(\mathbf{R}_\pm, du/|u|)$ into $L^2(\mathbf{R}_\pm, d\omega)$. If we assume that $D(x,y)$ has finite energy, i.e., if

$$\int_{-\infty}^\infty dx \int_0^\infty dy\,|D(x,y)|^2 < \infty \tag{3.B.10}$$

then it may be shown that the operators corresponding to $T_\pm(\cdot,\cdot)$ are compact operators. Hence these operators admit a singular value decomposition. In particular, it follows that the best approximations to either $T_+(\omega,u)$ or $T_-(\omega,u)$ using M functions $S_{\pm_n}(u)$, $n = 1,M$ and their corresponding echoes (images under $T_\pm(\cdot,\cdot)$) $E_{\pm_n}(\omega)$ is obtained by choosing the functions $S_{\pm_n}(u)$, $n = 1,M$ to be the singular functions of $T_+(\omega,u)$ or $T_-(\omega,u)$ corresponding to their M largest singular values. Note that since the singular functions $S_{\pm_n}(u)$ of $T_\pm(\cdot,\cdot)$ belong to $L^2(\mathbf{R}_\pm, du/|u|)$ they are the *Fourier transforms of valid wavelet functions*. Specifically, we have

$$\int_0^\infty \frac{|S_{\pm_n}(|u|)|^2}{|u|}du < \infty \tag{3.B.11}$$

which is the admissibility condition for wavelet functions.

Hence, if $D(x,y)$ is known, the best 2 norm approximation to it that uses N waveforms and their corresponding echoes can be computed by choosing a set of N waveforms from the set of $2N$ singular functions of $T_+(\omega,u)$ and $T_-(\omega,u)$ corresponding to their N largest singular values. The precise choice is made by computing the reduction that will occur in the norm of the error by including a particular singular function of $T_+(\omega,u)$ versus one of $T_-(\omega,u)$. The singular functions are considered in the order in which their corresponding singular values appear when arranged in order of decreasing magnitude.

3.B.3 Reconstruction of an unknown $D(x,y)$

The results of the last section provide a general guideline for choosing N waveforms for optimal reconstruction of a range-Doppler distribution $D(x,y)$. Specifically, the waveforms should be close approximations to the singular functions of $T_+(\omega,u)$ and $T_-(\omega,u)$ corresponding to their N largest singular values. The problem of course is that $D(x,y)$ is unknown.

It turns out that it is possible to find a set of functions that would act as approximate singular values for all kernels $T_+(\omega,u)$ and $T_-(\omega,u)$ that correspond to finite support range-Dopple densities $D(x,y)$. In particular, if the Fourier transforms $S_{\pm_n}(u)$ are chosen such that each $S_{\pm_n}(\ln(u))$ is equal to a particular translate and dilate of the same discrete wavelet function with a large number of vanishing moments then they will provide a good approximation to the singular functions of all kernels $T_+(\omega,u)$ and $T_-(\omega,u)$ that correspond to finite support range-Dopple densities $D(x,y)$ [58].

We still need to impose an ordering on these approximations to the singular functions of the kernels $T_+(\omega,u)$ and $T_-(\omega,u)$ that we expect to encounter. Specifically, we are really interested in approximating the singular functions of $T_+(\omega,u)$ and $T_-(\omega,u)$ corresponding to their *largest singular values*. This can again be done using the fact that $D(x,y)$ has a finite support in the (x,y) plane. The finite support constraint implies that $\Delta(\omega,y)$ is a smooth function in ω (its Fourier transform with respect to ω is a "low pass" function) and has a finite support in the y variable. This fact enables us to predict the asymptotic behavior of the wavelet coefficients in a 2-D discrete wavelet decomposition of either $T_+(\omega,u)$ or $T_-(\omega,u)$ [10].

More generally, if we can collect data corresponding to several representative $D(x,y)$ profiles we may use the following two step adaptive range-Doppler imaging scheme. In the first step we classify the available $D(x,y)$ densities into several classes using a clustering algorithm based on a norm criterion, e.g. the 2- norm. Next, for each class we compute a set of N waveforms that act as approximations to the singular functions corresponding to the largest singular values of the kernels $T_+(\omega,u)$ and $T_-(\omega,u)$ in this class. We also construct a set of N fixed waveforms to be used in a pre-imaging classification step. We will refer to these waveforms as the classification waveforms. This first step is

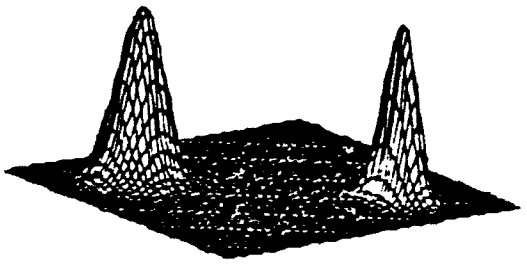

Figure 12: Actual $D(x, y)$

done *off-line*.

The second step is performed *on line* during actual imaging of a target. The radar first transmits the classification waveforms. A vector quantization routine then uses the approximate $D(x, y)$ reconstructed using these waveforms to determine the class of range-Doppler densities to which the observed $D(x, y)$ belongs. The radar finally transmits the appropriate set of waveforms corresponding to the identified class to obtain a higher resolution image of $D(x, y)$. The details of this procedure are given in [58].

3.B.4 A Simulation Example

Let us illustrate the above technique with a simple example. Assume that it is desired to image the distribution $D(x, y)$ shown in Fig. 12. This distribution consists of two 2-D Gaussian functions. The optimal reconstructions that we can obtain by sending one or two properly chosen wavelets are shown in Figs. 13 and 14. Note that Fig. 14 is essentially $D(x, y)$. This is the case because $D(x, y)$ is actually a rank 2 kernel. Hence, it can be reconstructed exactly using two properly chosen waveforms.

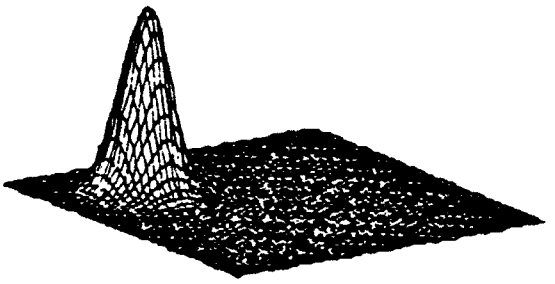

Figure 13: Reconstructed $D(x, y)$ Using 1 Wavelet.

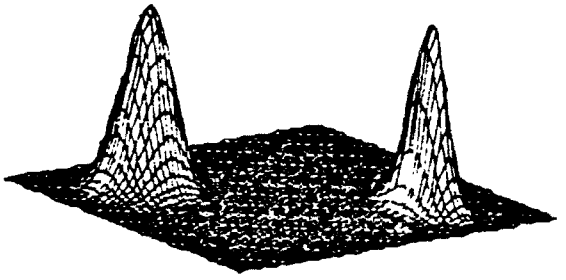

Figure 14: Reconstructed $D(x, y)$ Using 2 wavelets.

3.C Signal reconstruction from an Arbitrary Sampling of Its Dyadic Wavelet Transform

Wavelet transform maxima and zero-crossings signal representations have been investigated in both image and speech processing areas. Specifically, such representations can be used for image edge detection and multiscale image edge representations [40, 38, 39], speech pitch detection [30], and auditory representation of acoustic signals [71].

It has been conjectured that such a signal representation is complete (or unique) [11, 40, 38, 39]. However, recently in [3, 4] some counter examples have been given to show the non-completeness of such representations. In particular, a necessary and sufficient condition of the completeness has also been given in [3, 4]. Unfortunately, checking this condition involves determining the rank of a matrix that can have a potentially large size. Therefore, this condition is not practical.

In our work, we gave a necessary and sufficient condition for the completeness of the discrete dyadic wavelet transform extrema (or zero- crossing) representation for discrete finite data length signals. These signals are most commonly used in practice. We showed that the uniqueness of such a representation depends only on the locations of the wavelet transform extrema (local maxima and minima). Hence, our results apply as well to any arbitrary sampling of a redundant dyadic wavelet transform. Furthermore, we explained why the conclusions in [1,2,3] hold for most of the signals except for some extreme cases like those in [4,5]. We discussed the numerical stability of sampled dyadic wavelet representations. Stability is important in the sense that a numerically unstable representation is useless from a practical point of view. Finally, we described a fast Fourier transform (FFT) based algorithm for recovering a signal from a complete arbitrary sampling of its dyadic wavelet transform.

3.C.1 Dyadic Wavelet transforms and Sampled Dyadic Wavelet transforms

A fast dyadic discrete wavelet transform for the discrete signal $f(n)$ is computed by passing $f(n)$ through a cascade of filter banks that consist of low-pass and high-pass filters $H_j(\omega) = H_0(2^j\omega)$ and $G_j(\omega) = G_0(2^j\omega)$ (c.f. Fig. 15). The decomposition is essentially similar to a discrete orthogonal wavelet decomposition in which all decimators have been moved to the last stage and then eliminated. The prototype filters $H_0(\omega)$ and $G_0(\omega)$ must satisfy certain conditions. In particular, $H_0(\omega)$ is a low-pass filter with a zero of some order at $\omega = \pi$, and $G_0(\omega)$ is a high-pass filter with a zero of same order at $\omega = 0$, and $|H_j(\omega)|^2 + |G_j(\omega)|^2 = 1$. Furthermore, $H_0(\omega)$ and $G_0(\omega)$ have no other zero on the unit circle.

It is obvious that this decomposition is redundant. For example, if we choose

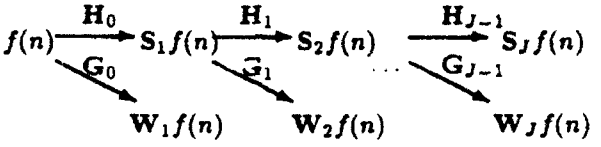

Figure 15: A Fast Dyadic Wavelet Transform.

the filters H_j and G_j such that they form a perfect reconstruction filter bank then we can decimate the filter outputs by a factor of two with no loss of information. The resulting decomposition is then called an orthonormal wavelet transform. Another approach given by Mallat [40, 38, 39] is to keep only the locations and the values of the local extrema or zero-crossings of $\mathcal{W}_j f(n)$ of the wavelet decompositions. We call such a signal representation a partial dyadic wavelet transform (PDWT) signal representation.

In our work, we analyzed the redundant wavelet transform of a finite size sequence $f(n)$. As is customarily done in this case, we assumed that the given sequence corresponds to a periodic signal with a period equal to the length of the given sequence. With this assumption, filtering signal $f(n)$ with $H_j(\omega)$ and $G_j(\omega)$ is equivalent to multiplying an $N \times 1$ vector $\vec{f}$ that consists of the N sample values of $f(n)$) with circulant matrices $\mathcal{H}_j$ and $\mathcal{G}_j$ of dimension $N \times N$. Specifically, denote by $\mathcal{W}_j \vec{f}$ the value of the discrete wavelet decomposition at scale 2^j. The $N \times 1$ dyadic wavelet transform vector $\mathcal{W}_j \vec{f}$ is obtained by multiplying the $N \times 1$ vector $\vec{f}$ of signal samples by the circulant matrix.

$$\mathcal{W}_j = \mathcal{H}_0 \cdots \mathcal{H}_{j-2} \mathcal{G}_{j-1}. \tag{3.C.1}$$

The smoothed version at scale 2^J is $\mathcal{S}_J \vec{f}$. It is equal to the product matrix,

$$\mathcal{S}_J \vec{f} = \mathcal{H}_0 \mathcal{H}_1 \cdots \mathcal{H}_{J-1} \vec{f}. \tag{3.C.2}$$

The properties of $H_j(\omega)$ and $G(\omega)$ imply that the rank of $\mathcal{S}_J$ is not N. Hence it is not possible to reconstruct $\vec{f}$ from $\mathcal{S}_J \vec{f}$. The question then is: "Is it possible to reconstruct $\vec{f}$ from a PDWT?" To answer this question, we write the PDWT of the signal representation as

$$\mathcal{W} \vec{f}. \tag{3.C.3}$$

Here the matrix $\mathcal{W}$ is called partial dyadic wavelet transform (PDWT) matrix and is defined as,

$$\mathcal{W} = \left[\mathcal{S}_J^T \mid \mathcal{W}_{1,p_1}^T \mid \cdots \mid \mathcal{W}_{J,p_J}^T \right]^T. \tag{3.C.4}$$

The vectors $p_j = [p_j(i)]$ consist of the indices of the samples of $\mathcal{W}_j \vec{f}$ that have been retained (e.g. the extrema locations m_j, or zero-crossing locations z_j) at

scale j. The matrices W_{j,P_j} consist of the rows of W_j corresponding to the locations in p_j.

The advantage of the above matrix form is that the PDWT problem can be directly studied by examining the matrix W. For example, the representation is complete, (that is, there exist no other signals $\vec{f}$ with the same representation $W\vec{f}$) if and only if rank of matrix W is N.

3.C.2 Completeness and stability of a Sampled Dyadic Wavelet transform

As noted above, the PDWT signal representation is said to be complete (or unique) if and only if there exist no other signal $\vec{g}$ other than $\vec{f}$ such that $W\vec{g} = W\vec{f}$. This completeness (or uniqueness) has been conjectured in [40, 38, 39] because no counter examples had been found. From our discussions in the previous section, the completeness of PDWT can be describe by the following lemma,

Lemma 1 *The PDWT signal representation is complete if and only if rank(W) = N.*

The proof to this lemma is obvious. Notice that a similar result has been derived in [3, 4]. As mentioned above, it is rather difficult to check the completeness of a PDWT using this Lemma because the size of W can be large.

Using the above lemma and the fact that the eigenvalues of an $N \times N$ circulant matrix C are the discrete Fourier transform coefficients of elements of C and the corresponding eigenvectors are the columns of the $N \times N$ Fourier transform matrix, we proved the following completeness theorem.

Theorem 1 *The PDWT representation is complete if and only if*

$$\sum_{j=1}^{J} \eta_j \geq 2^J - 1. \tag{3.C.5}$$

where

$$\eta_j = \begin{cases} \text{the number of distinct values } p_j(i) \bmod 2^J \\ \qquad\qquad \text{for } 1 \leq j \leq J-1 \\ \text{the number of distinct values } p_J(i) \bmod 2^{(J-1)} \\ \qquad\qquad \text{for } j = J \end{cases} \tag{3.C.6}$$

We outline here the main argument used to prove this result. Since $\mathbf{S}_J(\omega) = H_0(\omega) \cdots H_{J-1}(\omega)$ has zeros of some order only at $\omega = \pi, \pm\frac{\pi}{2}, \cdots, \pm\frac{\pi}{2^{J-1}}$,

$$\text{rank}(S_J) = N - 2^J + 1. \tag{3.C.7}$$

The eigenvectors corresponding to the zero eigenvalues of S_J would be $\vec{\mathcal{F}}(\frac{N}{2}), \vec{\mathcal{F}}(\pm\frac{N}{4}), \cdots, \vec{\mathcal{F}}(\pm\frac{N}{2^J})$, where the $N \times 1$ Fourier vector $\vec{\mathcal{F}}(n)$ is defined as

$$\vec{\mathcal{F}}(n) = \left[1, e^{-j2\pi\frac{n}{N}}, \cdots, e^{-j2\pi\frac{n(N-1)}{N}}\right]^T \tag{3.C.8}$$

Since the information in $\vec{f}$ that was lost in $S_J\vec{f}$ should be present in

$$\mathcal{W}_p\vec{f} = \left[\mathcal{W}_{1,p_1}^T \mid \cdots \mid \mathcal{W}_{J,p_J}^T\right]^T \vec{f}, \tag{3.C.9}$$

the matrix,

$$\mathcal{W}_p\left[\vec{\mathcal{F}}(-\frac{N}{2^J}), \cdots, \vec{\mathcal{F}}(\frac{N}{2^J})\right] \tag{3.C.10}$$

should have rank $2^J - 1$ to guarantee completeness. This argument serves as the basis of the proof of the above Theorem. The detailed proof can be found in [76].

The above Theorem is important because it provides us with a simple way of checking the completeness of any sampled dyadic wavelet representation. In particular, our test does *not* involve computing the rank of any matrix.

Up to this point, we discussed the signal compensation of the smoothed signal $S_J\vec{f}$ corresponding to the zero eigenvalues of S_J. To guarantee the numerical stability of PDWT representation, we need to consider also the eigenvalues of S_J of negligible magnitude. By slightly modifying the above theorem, one can derive a similar condition on the number and location of the samples that are retained to guarantee a unique and numerically well behaved representation. We refer the interested reader to [76] for more details.

We give here a simulation result. Fig. 16 shows a wavelet $\psi(x)$ and its scaling function $\phi(x)$. Fig. 17 shows a signal $\vec{f}$ equal to a row in an image and its wavelet transform up to scale $J = 4$ by using the wavelet given in Fig. 16. Fig. 18 shows the maxima representation of the wavelet transform in Fig. 17. We can examine the sampling locations of local maxima using the theorem and conclude that the representation is complete. Next, we detect the "edge" of the image row, that is, keep only the samples corresponding to the same maxima locations at all scales as shown in Fig. 19. Using the completeness theorem, we find that the representation is still complete.

3.C.3 Signal Reconstruction from a Sampled Dyadic Wavelet transform

The problem now becomes how to reconstruct the original signal $\vec{f}$ from the PDWT representation $\mathcal{W}$. The above discussion gives rise to an FFT based reconstruction algorithm. In particular, the original signal $\vec{f}$ can be reconstructed as follows from a PDWT

$$\vec{f} = \mathcal{W}^\dagger\mathcal{W}\vec{f}. \tag{3.C.11}$$

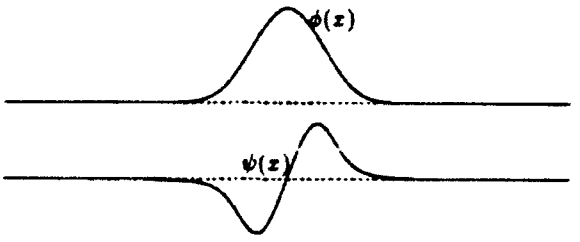

Figure 16: Scaling Function $\phi(x)$ and Wavelet $\psi(x)$.

In the above equation where $\mathcal{W}^\dagger$ denotes the pseudo inverse of $\mathcal{W}$. Typically, the above equation will be difficult to be implement because of the possibly large size of $\mathcal{W}$.

Instead of using (3.C.11) we may proceed as follows. First, we recover the information about $\vec{f}$ that is in $S_J\vec{f}$. Specifically, we construct an approximation $\vec{f}_s$ to $\vec{f}$ as

$$\vec{f}_s = Q^H \text{diag}\{\tilde{S}_J(0), \cdots, \tilde{S}_J(N-1)\} Q S_J \vec{f}. \tag{3.C.12}$$

In the above equation Q denotes the $N \times N$ Fourier transform matrix and Q^H is its complex conjugate transpose. The diagonal entries $\tilde{S}_J(n)$ are given by

$$\tilde{S}_J(n) = \begin{cases} \frac{1}{S_J(n)} & \text{if } S_J(n) \neq 0 \\ 0 & \text{otherwise.} \end{cases} \tag{3.C.13}$$

The difference $\vec{f}_e$ between $\vec{f}$ and $\vec{f}_s$ is then finally obtained as

$$\vec{f}_e = \mathbf{F}(\mathcal{W}_p\mathbf{F})^\dagger(\mathcal{W}_p(\vec{f} - \vec{f}_s)) \tag{3.C.14}$$

where

$$\mathbf{F} = \left[\vec{\mathcal{F}}(-\frac{N}{2^J}), \cdots, \vec{\mathcal{F}}(\frac{N}{2^J})\right] \tag{3.C.15}$$

and $A^\dagger$ denotes the pseudo inverse of A. The advantage of this representation is that it involves solving for $2^{J-1} - 1$ unknowns only.

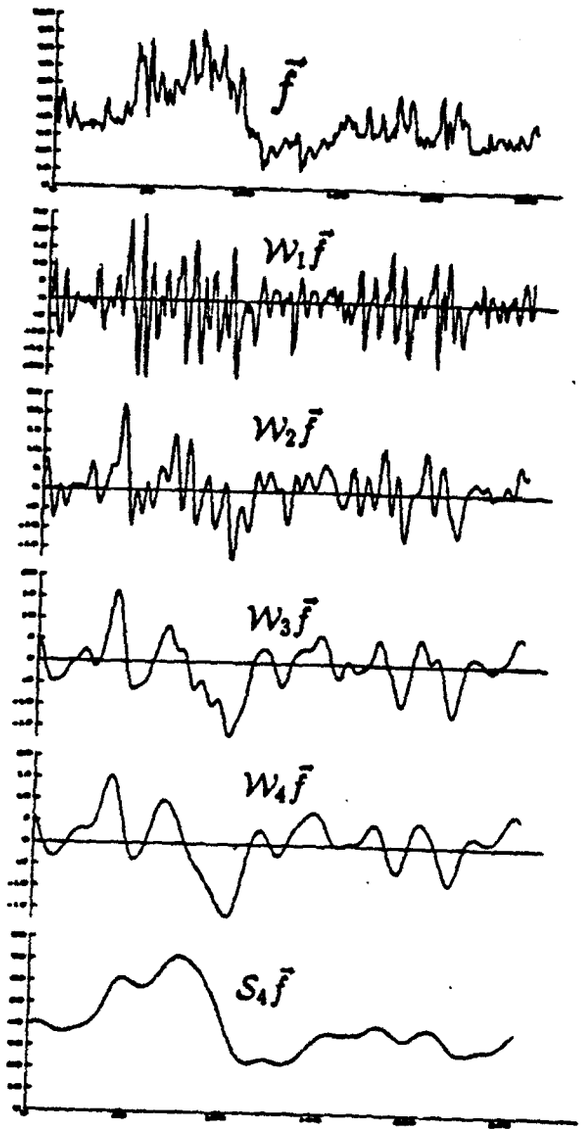

Figure 17: Dyadic Wavelet Transform up to Scale J=4.

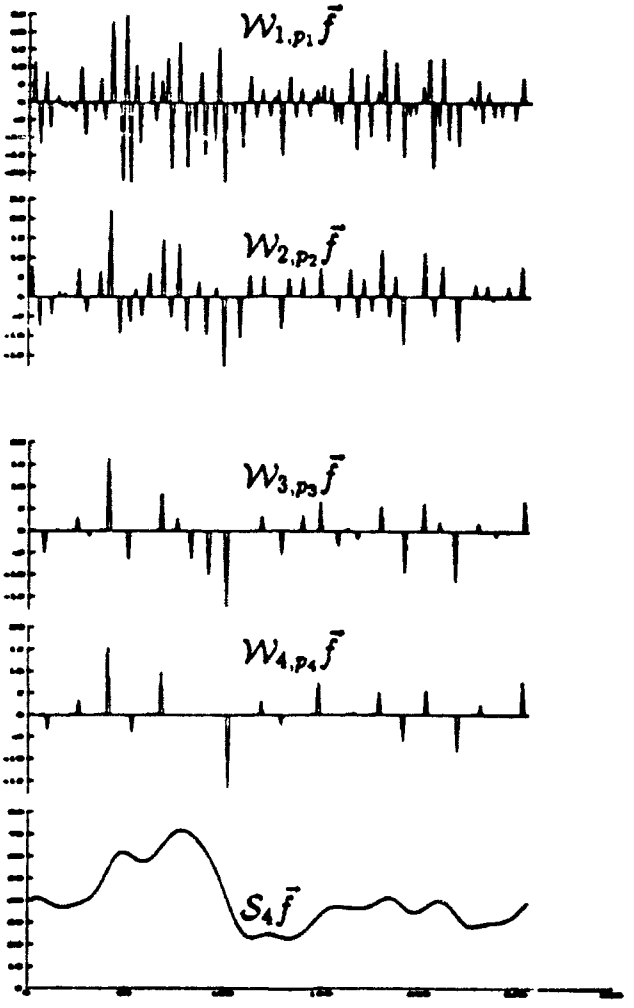

Figure 18: Wavelet Transform Extrema Representation of $\vec{f}$.

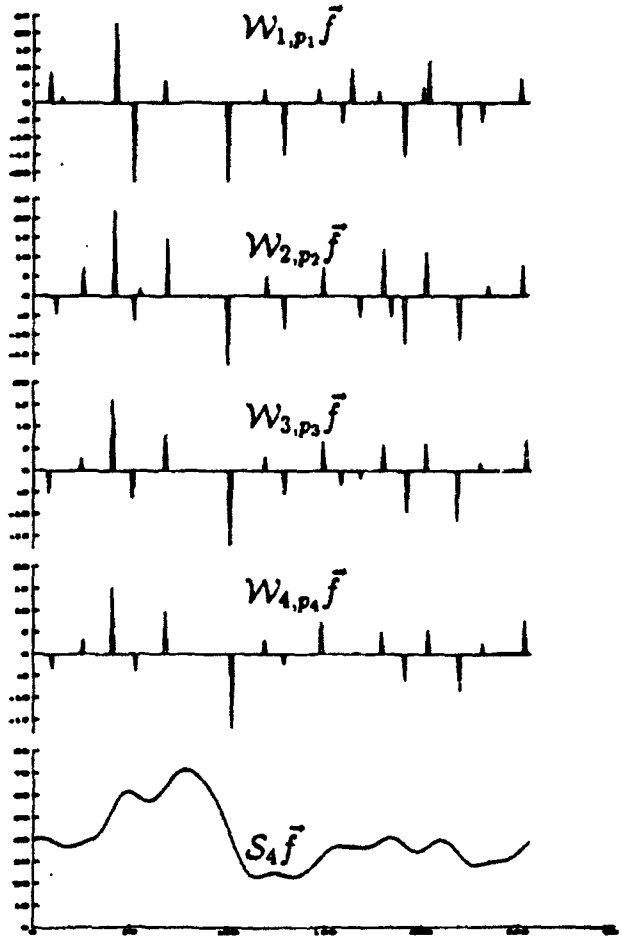

Figure 19: A More Efficient Sampled Wavelet Transform Representation of $\vec{f}$.

3.D Adaptive wavelet Representations for Low Bit Rate High Quality Audio Coding

In many application, such as the design of multimedia workstations and high quality audio transmission and storage the goal is to achieve transparent coding of hi-fidelity audio signals at bit rate below 64 kb/s. Typically, the quality of Compact Disk(CD) signals is used as the standard for high fidelity. These signals are characterized by a high bandwidth (sampling rate of 44.1kHz), and a high quality (16 bits/sample PCM coding), resulting in a high bit rate of 705 kb/s. Reducing this requirement while maintaining a near transparent quality is, therefore, crucial in the above applications.

In other applications the objective is to synthesize music signals at or below 10 kb/s. The transform and subband coders have generally been found to be unsuitable at these rates and the low bit rate speech coders are almost invariably based on the Linear Predictive Coding (LPC) algorithms or its extensions. Since the LPC model relies on the human voice production mechanism, it may not be suitable for music and other non-speech sounds. (Note that, some studies suggest that Multi Pulse LPC may be viable for this task [50].)

In general, an audio coding scheme must exploit irrelevancies (which result from the masking properties of human hearing) and statistical redundancies in the signal. The currently known methods for hi-fi audio compression [66],[29], generally concentrate on exploiting the masking properties by looking at a suitable transform or subband components of the signal. We proposed an audio coder that attempts to maximize the compression by utilizing both the above sources of redundancies in a signal. To exploit masking a discrete wavelet transform (DWT) based Adaptive Transform Coding method is employed. The DWT is attractive for audio compression because it acts like a Karhunen Loeve Transform (KLT) for a large class of signals (including some non-stationary signals) [61]. Furthermore, it offers the flexibility of choosing a basis matched to the given data. The proposed coder incorporates an *optimal* wavelet basis search procedure to utilize this flexibility. The DWT part of the coder builds on our previous work [51]. With recent improvements, it is capable of maintaining a near transparent quality at approximately 64 kb/s.

To eliminate the statistical redundancies in the signal, the DWT encoder is augmented by a first stage of dynamic dictionary based encoding. Experiments with several audio samples suggest that this results in a significant coding gain. The overall two-stage coder offers a solution to first of the audio compression problems noted above; i.e., it allows transparent coding of CD quality audio signals at rates below 64 kb/s. Preliminary studies suggest that it is also a viable approach for the low bit rate synthesis of music signals at about 10 kb/s.

It should also be noted that the decoding part of this algorithm has been implemented in real time on a Texas Instruments, TMS320C31 chip. The coder complexity is still high, even though significant speedup in the wavelet adaptation algorithm has been achieved. Also, the coder in its present form leads to a

variable data rate. The implementation of our procedure may therefore require the use of a buffering scheme in some practical applications.

3.D.1 Particulars Of The Audio Compression Method

The overall coding algorithm is illustrated in Figure 20. In what follows, we assume that the incoming stream of audio data has been sampled at 44.1 kHz. It is divided into short frames. For each of these frames a dictionary entry that is perceptually closest to the signal is identified. The chosen entry is then subtracted from the signal to form an error vector. Both the signal and the error are encoded using an optimal WT based approach, and shorter of the two codes is transmitted to the receiver.

The audio coder uses two different analysis frame sizes of 1024 and 2048 samples (46 and 23 ms). The ends of these frames are tapered by the square-root of a Hanning window, the resulting overlap corresponds to an oversampling ratio of 6.67%. The longer frame results in lower bit rates and is, therefore, employed most of the time. The shorter frame length, on the other hand, is used for frames which are identified to be susceptible to the "pre-echo" effect, based on an "energy-entropy" criterion described in a later section. It may be noted that neither of the two frame sizes provide the time resolution determined by backward masking of sharp transients, i.e., 4 ms. But, the proposed coder contains additional safeguards against pre-echos and these are also described in a later section.

3.D.2 Discrete Wavelet Transformation of Audio Frames

The classical formulation of DWT leads to "octave bandwidth" filterbanks, i.e., filter bandwidth is proportionately higher for the high frequency bands. Frequency resolution of such filterbanks does not quite match the frequency dependent resolution required for full exploitation of simultaneous masking (i.e., the "critical band" structure [29]). To alleviate this problem, we used the wave packet representations [14]. In such a representation, the low and high frequency bands are further split. This representation retains the flexibility offered by the DWT in terms of choosing an optimal basis. The wave-packets may be used to form any arbitrary binary tree structured decomposition. In our work we use a tree containing a maximum of 29 bands that closely resembles the critical band scale.

3.D.3 Perceptual Masking Constraint in the Wavelet Transform Domain

Perceptual masking or simultaneous masking is a phenomenon whereby a strong signal masks a simultaneously occuring weak (noise) signal. The importance of masking in a coding system is that a perceptually transparent quality

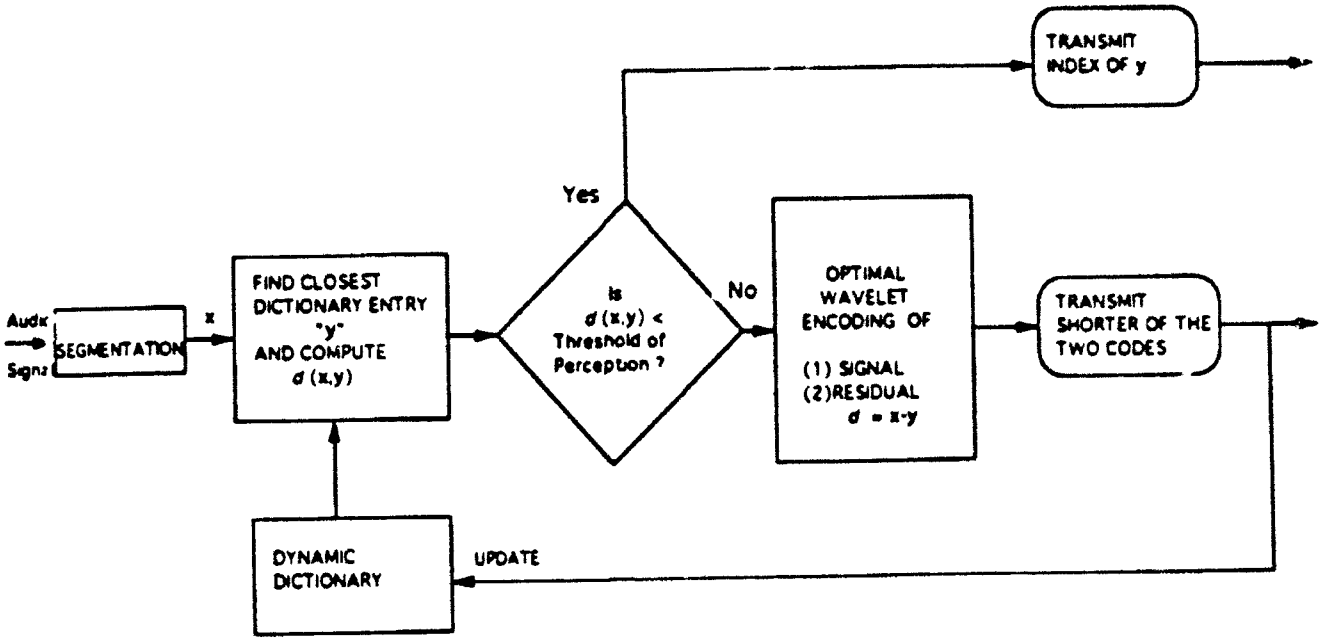

Figure 20: Block diagram of the proposed coder

is maintained as far as the power of reconstruction error in each of the critical bands is below a signal dependent threshold. In our computations of the noise masking threshold, we use the following particulars: FFT analysis for windowed signal frame, assumption of additivity for the masked power, and a model for inter/intra frequency masking proposed in [66]. Additionally, the threshold is forced to be constant for each of the wavelet (critical) bands.

Under the assumption that the transform coder "whitens" the quantization error (which turns out to be the case), the threshold of masking may be enforced by

$$\mathbf{e}_\mathbf{q}^* \mathbf{R}_\mathbf{Q} \mathbf{e}_\mathbf{q} \leq D \tag{3.D.1}$$

where $\mathbf{e_q}$ is the error vector in the quantization of DWT coefficients, D is a threshold, and $\mathbf{R_Q}$ is a positive definite matrix which depends on the choice of the wavelet. In general this matrix is not diagonal. However, in [53] we show that if the analyzing wavelet has a large number of vanishing moments then $\mathbf{R_Q}$ is very close to being diagonal. Then the error criterion (1) reduces to

$$\sum_k c_{kk}(\Theta) e_k^2 \leq D \tag{3.D.2}$$

where Θ is a vector of parameters that identifies the selected wavelet, e_k is the error in the k^{th} WT coefficient, and $c_{kk}(\Theta)$ is the k^{th} diagonal entry of $\mathbf{R_Q}$. The WT domain threshold $c_{kk}(\Theta)$ remains constant for a particular subband [53].

3.D.4 Audio Data Compression By Wavelet Optimization

In our code, an optimal wavelet is identified for each frame of the audio signal (N samples) and the bits are optimally allocated among the different WT coefficients to minimize the overall bit rate requirement. In [53], we show that for a particular choice of a wavelet, the minimum number of bits for quantizing the WT coefficient is given by (assuming a large number of vanishing moments for the wavelet),

$$R_{min}(\Theta) = \frac{1}{2}\sum_{k} \log_2 \frac{\sigma_k^2 c_{kk}(\Theta)}{C} \qquad (3.D.3)$$

where σ_k is the peak value of the k^{th} coefficient (if a uniform adaptive quantizer is employed), and the constant $C = \frac{D}{\epsilon N}$ (ϵ is a "safety factor" close to 1). The k^{th} term in the above summation also gives the optimum bit allocation, R_k^{opt}, for the k^{th} WT coefficient. For a particular choice of a wavelet, the bit rate requirement may then be computed directly from the transform coefficients using the above equation.

If an attempt is made to identify the best wavelet by searching in the parameter space, the overall search complexity can be extremely high. In [53], we conclude that for longer scaling sequences (of size K), the search may be limited to the set of wavelets with maximal number ($K/2$) of vanishing moments, with near optimal results. The families of K coefficient $K/2$ vanishing moment wavelets are generated using the results in [17] (e.g., for $K = 20$, there are exactly 1024 such wavelets). Furthermore, a fast search procedure may be developed using the fact that all K coefficient $K/2$ vanishing moment wavelets result in filter banks with identical magnitude response; these differ only in terms of their phase responses (delay). The fast algorithm significantly reduces the complexity of search by limiting the optimization to the last stage of the wavelet decomposition tree.

The information that needs to be transmitted to the receiver to recompute bit allocation is $\{\sigma_k, c_{kk}\}_{k=1}^{k=N}$, and the choice of the wavelet Θ. It was noted earlier that only 29 values of c_{kk} need to be transmitted. these are quantized uniformly on a log scale using 6 bits and a resolution of 1.3 dB. Transmitting the peak values σ_k too frequently leads to excessive side information. In our work, updating these values once every 8 transform coefficients was found to be a suitable compromise. The peak values are quantized using a simple mean-difference quantizer at 2 bits/value. Identifying the best, maximal vanishing moment wavelet requires only a small number of bits per frame. The overall side-information for the WT based coder requires approximately 0.3 bits/sample.

3.D.5 Dynamic Dictionary Based Encoding

Although the wavelet based coding method is able to exploit the masking characteristics, further reduction in the bit rate is possible by getting rid of the statistical redundancies. One possible way to do that is to use predictive

coding (differential PCM). However, this method has generally been found to be unsuitable for maintaining transparent quality across a wide range of hi-fi music signals. Another possibility is to use vector quantization (VQ) [24]. It has been shown that VQ coders are theoretically superior in the sense that the rate distortion bounds on the data rate are better achievable than with scalar quantization. Still, VQ has found only a limited role in hi-fi audio coding because of lingering doubts about its ability to ensure transparent quality. Significant among the previous attempts towards using a VQ for audio compression is the work by Chan and Gersho [12]. It employs a fixed multi-stage tree structured codebook trained on DCT coefficients.

In our work, in an attempt to guarantee transparent quality for all type of audio signals, we use a dynamic system as illustrated in Figure 1. It employs an adaptive dictionary in a first stage of VQ for the audio waveform. At the same time the difference between the audio waveform and the chosen dictionary entry is also encoded using the wavelet based method discussed above. Using this second coding stage allows us to use a dictionary of relatively small size and rather simple methods for dictionary construction and update. However, even under these conditions the use of VQ as a first stage results in significant coding gain.

In Figure 20, the DWT encoding procedure for the residual remains exactly the same as the one for the signal itself (as described above). Moreover, perceptual threshold for the coding of the difference signal is also the same as the perceptual threshold of the signal itself. This is because the coding errors in $\mathbf{x}$ are exactly equal to the errors in the quantization of residual, $\mathbf{d}$. On the other hand, the dictionary encoding procedure works as follows. Each frame of audio data is split into two halves (unless the frame length has already been halved for pre-echo control). For either of the two half frames the dictionary is searched for the best perceptual matches using a procedure described below. The best entries are then subtracted from the respective halves of the signal $\mathbf{x}$ to form the residual vector $\mathbf{d}$.

Dynamic Dictionary Search

Given a normal frame length of N samples, the above discussion indicates that the dictionary is used to encode vectors of $N/2$ samples. The dictionary entries, however, are maintained as "meta vectors" of N samples each. To encode a signal $\mathbf{x}$ we search through the dictionary to find an element μ_o which is closest to $\mathbf{x}$ in terms of a "perceptual distance measure". This distance is computed by executing the following three steps

1. Compute a sliding window correlation between $\mathbf{x}$ and μ and find the lag L_i corresponding to the peak of the correlation function ($0 \leq i \leq N/2$). Next, form a vector $\mathbf{y}_o$ consisting of $N/2$ samples of μ starting from lag L_i.

2. Estimate the time warping factor to normalize the time scale of of $\mathbf{y}_o$ to that of $\mathbf{x}$ (see below).

3. Compute a frequency weighted error for the error vector $\mathbf{e} = \mathbf{x} - \mathbf{y}_o$ using the perceptual threshold computed from $\mathbf{x}$. This error power is the requisite perceptual distortion measure.

Step 1 and 2 above ensure a better perceptual match through an improved time and scale alignment. The incorporation of these steps increases the effective size of the dictionary significantly beyond its physical dimension.

Time Warp Factor Estimation

In the dictionary based encoding it is often useful to renormalize the time scale of the dictionary entry to that of the signal. However, in the audio coder an exact characterization of a warping function is not an important issue (unlike the speech/speaker recognition systems), *since residuals are also being transmitted simultaneously*. Thus, it may be assumed that there is a constant time-warp factor for the entire frame of audio data. In [53], we show that a warp factor α that minimizes $\int [x(t) - y(\alpha t)]^2 dt$, may be estimated as

$$\gamma = \frac{\sum_k k[x(k) - y(k)].[y(k+1) - y(k)]}{\sum_k k^2[y(k+1) - y(k)]^2}. \qquad (3.D.4)$$

where $-0.5 \leq \gamma \leq 0.5$, and $\alpha = 1 + \gamma$.

Dynamic Dictionary Update

An adaptive dictionary has previously been used in some applications, e.g., for for image compression [22]. The dictionary update problem in the proposed coder is somewhat different because dictionary entries consist of waveforms and the vector sizes are relatively large making it impractical to collect several samples before executing an update step. Since the proposed encoder also encodes the residual, we have so far been able to work with a simple dictionary update procedure as follows. The minimum distance measure between $\mathbf{x}$ and perceptually closest entry into the dictionary is compared against a preselected threshold. If it is below the threshold then the dictionary remains unchanged, otherwise the decoded signal $\hat{\mathbf{x}}$ is used to update the dictionary using a Longest-Time-Since-Use strategy. Several improved techniques for dictionary update in the audio coder are currently under investigation. These are based on adaptive filtering/multigrid adaptive filtering algorithms.

3.D.6 Adaptive Framing for Pre-echo Control

It was noted earlier that a longer analysis frame size of 2048 samples is desirable for lower bit rates. But, using a large frame size implies that reconstruction errors are spread over the effective width of the window in time. The backward masking of an impulse lasts about 4 ms and is not sufficient to mask the error spectrum for the full duration of a longer frame. This leads to the pre-echo effect in the presence of a sudden increase (impulse) in the signal energy. To limit pre-echos, the coder switches to a shorter frame size (1024 samples) whenever presence of strong transients is detected based on an *energy- entropy* estimate

(computed as follows). Each frame is divided into segments of J ($J = 16$ is a suitable value at 44.1KHz) samples each. Signal energy, σ_i, is computed over each of these segments and is normalized by the overall frame energy. We then define energy-entropy as

$$I = -\sum_i \sigma_i^2 \log_2 \sigma_i^2. \tag{3.D.5}$$

This entropy measure falls sharply for segments with sudden bursts of energy. An entropy value of 4.5 bits is used as a threshold for switching the frame size.

The shorter frame eliminates pre-echos to a significant extent. Further reduction in pre-echos is accomplished by utilizing the time varying signal energy estimate available in the form of peak-values. These peak-values are used to scale the WT domain masking threshold for the frames in which presence of sharp transients is detected based on the above entropy criterion.

3.D.7 Experimental Results

The proposed audio coder was tested using a database of several audio samples (castanets, piano, pop, drums, clarinet, etc.). For each sample a perceptually transparent coding (at variable bit rates) was attempted. The bit rates in the DWT based coder were found to be in the range of $0.8 - 1.2$ bits/sample for coding the transform coefficients. When a dynamic dictionary of 150 entries was employed, the coefficients could be encoded at the rates of $0.6 - 1.0$ bits/samples. Including the side information (about 0.3 bits/sample), these figures correspond to bit rates close to 64 kb/s or below for the DWT based method alone and in the range of $48 - 64$ kb/s with the dictionary encoding.

The subjective quality in "transparent" coding by the proposed coder was assessed by comparing the quality of transcoded samples with that of MPEG layer-2 coding [7] of the same samples. In listening tests, trained listeners were unable to detect any difference between the original and the transcoded samples (of the proposed coder). In the judgement of some listeners the quality of 64 kb/s wavelet coding was better than 128 kb/s MPEG layer-2 coding.

A detailed description of our tests and test results may be found in [53].

4 PERSONNEL

- Principal Investigator
  1. Prof. A. H. Tewfik
- Graduate Students
  1. Deepen Sinha
  2. Hehong Zou

5 JOURNAL PUBLICATIONS

1. "Low Bit Rate Transparent Audio Compression Using Adapted Wavelets," D. Sinha and A. H. Tewfik, to appear in *IEEE Trans. on Signal Proc.*, Dec. 1993.

2. "Signal Reconstruction from a Sampled Dyadic Wavelet Transform Representation," H. Zou, A. H. Tewfik and W. Xu , submitted to *IEEE Trans. on Signal Proc.*, April 1993.

3. "Waveform Selection for High Resolution Radar Range- Doppler Imaging" A. H. Tewfik, in preparation, to be submitted to *IEEE Trans. on Image Proc.*, April 1993.

4. "Wavelet Domain Bearing Estimation" A. H. Tewfik , in preparation, to be submitted to *IEEE Trans. on Signal Proc.*, 1993.

6 INVITED CONFERENCE PUBLICATIONS

1. "Robust Wavelet Domain Array Processing," A. H. Tewfik and M. Kim, invited paper, in *Proc. 6h IEEE Signal Proc. Workshop on Statistical Signal and Array Proc.*, Victoria, B. C., Canada, Sept. 1992.

2. "Wavelets in Optimal Radar Range-Doppler Imaging," A. H. Tewfik, invited paper, in *Proc. 26th Asilomar Conference on Signals, Systems and Computers*, Monterey, CA., Oct. 1992.

3. "Estimation of Range-Doppler Radar Images," A. H. Tewfik, invited paper, in *Proc. of the 1993 IEEE Symp. on Circuits and Systems*, Chicago, IL, May 1993.

4. "Acoustical Applications of Wavelets: Sonar and Audio Coding." A. H. Tewfik, invited paper, in *Proc. 125th Meeting of the Acoustical Society of America*, Ottawa, Canada, May 1993.

7 CONFERENCE PUBLICATIONS

1. "Complete Discrete Wavelet Transform Extrema Representations," H. Zou, A. H. Tewfik and W. Xu, in *Proc. of the Fifth Digital Processing Workshop*, Starved Rock State Park, IL, Sept. 1992.

2. "Optimal Waveform Selection in Range-Doppler Imaging," A. H. Tewfik in Proc. of the Fifth Digital Processing Workshop, Starved Rock State Park, IL, Sept. 1992.

3. "Completeness and Stability of Partial Wavelet Domain Signal Representations" H. Zou, A. H. Tewfik and W. Xu , in *Proc. of the 1993 IEEE Conf. on Acoust. Speech and Signal Proc.*, Minneapolis, MN, April 1993.

4. "Low Bit Rate Transparent Audio Compression Using a Dynamic Dictionary and Optimized Wavelets" D. Sinha and A. H. Tewfik, in *Proc. of the 1993 IEEE Conf. on Acoust. Speech and Signal Proc.*, Minneapolis, MN. April 1993.

8 INTERACTION WITH AIR FORCE LABORATORIES

- *Rome Air Defense Center, Rome, NY*: Seminar on "Wavelet Techniques in Surveillance Systems", September 1992.

References

[i] A. J. Barabell, "Improving the Resolution Performance of Eigenstructure Based Direction-Finding Algorithms," in *Proc. 1983 Int. Conf. on Acoust. Speech and Signal Proc.*, Boston, MA, pp. 336-339, 1983.

[2] R. J. Barton and H. V. Poor, "Signal Detection in Fractional Gaussian Noise," *IEEE Trans. on Info. Theory*, vol. IT-34, no. 5, pp. 943-959, 1988.

[3] Z. Berman, "The Uniqueness Question Of Discrete Wavelet Transform Maxima Representation", *Tech. Report TR 91-48r1, Univ. of Maryland*, April 1991.

[4] Z. Berman, "A Reconstruction Set Of A Discrete Wavelet Transform Representation", *Proc. of IEEE Intern. Conf. Acoust. Speech and Signal Proc.*, San Francisco, March 1992.

[5] M. Bernfeld, "Chirp Doppler Radar," *Proc. IEEE*, vol. 72, no. 4, pp. 540-541, 1984.

[6] G. Beylkin, R. Coifman, and V. Rokhlin, "Fast Wavelet Transforms and Numerical Algorithms I," *Comm. on Pure and Appl. Math.*, vol. 44, pp. 141-183, March 1991.

[7] K. Brandenburg, G. Stoll et. al., "The ISO-MPEG-Audio Codec: A Generic-Standard for Coding of High Quality Digital Audio," Preprint, *Journal of the Audio Engineering Society*, 1992.

[8] W. S. Burdic, *Underwater Acoustic System Analysis*, Prentice Hall Inc., Englewood Cliffs, N.J. 1984.

[9] A. Calderon, "Intermediate Spaces and Interpolation: The Complex Method," *Studia Math*, vol. 24, pp. 113-190, 1964.

[10] A. Calderon and A. Torchinsky, "Parabolic Maximal Functions Associated to a Distribution, I," *Adv. Math.* vol. 16, pp. 1-64, 1975.

[11] A. Cetin and R. Ansari, "Signal Recovery from Wavelet Transform Maxima", pre-print, submitted to *IEEE Trans. on Signal Processing.*, Sept. 1991.

[12] W. Y. Chan and A. Gersho, "High Fidelity Audio Transform Coding with Vector Quantization," *Proc. 1990 Int. Conf. Acoust, Speech and Signal Proc.* pp. 1109- 1112, April 1990.

[13] A. Cohen and I. Daubechies, "Non-Separable Bidimensional Wavelet Bases," preprint.

[14] R. R. Coifman, Y. Meyer, S. Quake and M. V. Wickerhauser, "Signal Processing and Compression with Wave Packets," preprint, Dept. of Mathematics, Yale Univ, 1990.

[15] C. E. Cook and M. Bernfeld. *Radar Signals*, New York: Academic Press, 1967.

[16] W. Dahmen and C. A. Micchelli, "Stationary Subdivision, Fractals and Wavelets", in *Computation of Curves and Surfaces*, W. Dahmen et al., eds, NATO ASI Series C: Mathematical and Physical Sciences, Kluwer Academic Publishers, 1990.

[17] I. Daubechies, "Orthogonal Bases of Compactly Supported Wavelets," *Commun. Pure Appl. Math.*, vol. 41, pp. 909-996, 1988.

[18] I. Daubechies, "Wavelet Transform, Time-Frequency Localization and Signal Analysis," *IEEE Trans. Info. Theory*, vol. 36, no. 5, pp. 961-1005, 1990.

[19] I. Daubechies and J. Lagarias, "Two Scale Difference Equations: Existence and Global Regularity of Solutions," *SIAM J. Math. Anal.*, vol. 22, no. 5, pp. 1388-1410, Sept. 1991.

[20] M. Deriche and A. H. Tewfik, "Maximum Likelihood Estimation of the Parameters of Discrete Fractals and Cramer-Rao Bounds," to appear in *IEEE Trans. on Signal Processing*, Oct. 1993.

[21] E. Feig and F. A. Grunbaum, "Tomographic Methods in Range-Doppler Radar," *Inverse Problems*, vol. 2, no. 2, pp. 185- 195, 1986.

[22] A. Gersho and M. Yano, "Adaptive Vector Quantization by Progressive Code Vector Replacement," *Proc. 1985 Int. Conf. Acoust, Speech and Signal Proc.*, pp. 133-136, 1985.

[23] G. H. Golub and C. F. Van Loan, *Matrix Computations*, Johns Hopkins Univ. Press, Baltimore, MD, 1983.

[24] R. Gray. "Vector Quantization," *IEEE Acoust. Speech and Signal Proc. Magazine*. pp. 4-29, April 1984.

[25] A. Grossman and J. Morlet, "Decomposition of Hardy Functions into Square Integrable Wavelets of Constant Shape," *SIAM J. Math.*, vol. 15, pp. 723-736, 1984.

[26] J. R. M. Hosking, "Fractional Differencing," *Biometrica*, 68.1, pp. 165-176, 1981.

[27] R. Hummel and R. Moniot, "Reconstruction from Zero-Crossings in Scale-Space", in *IEEE Trans. Acoust. Speech and Signal Proc.*, vol. ASSP-37, no. 12, pp. 2111-2131, Dec. 1989.

[28] S. Jaffard, "Estimations Holderiennes Ponctuelles Des Fonctions Au Moyen Des Coefficients D'Ondelettes," in *notes au comptes Rendu de l'Academie des Sciences*, France, 1989.

[29] J. D. Johnston, "Transform Coding of Audio Signals Using Perceptual Noise Criteria", *IEEE Journal on Selected Areas in Communications*. Vol. 6, pp. 314-323, 1988.

[30] S. Kadambe and G. F. Boudreaux- Bartels, "Application of the wavelet transform for the pitch detection of speech signals," *IEEE Trans. on Info. Theory*, vol. 38, no. 2, pp. 917-924, March, 1992.

[31] S. M. Kay, *Modern Spectral Estimation*, Prentice-Hall, 1988.

[32] E. J. Kelly and R. P. Wishner, "Matched Filter Theory for High Velocity Accelerating Targets," *IEEE Trans. Mil. Electronics*, vol. MIL-9, pp. 56-69, 1965.

[33] J. Kovacevic and M. Vetterli, "Nonseparable Multidimensional Perfect Reconstruction Filter Banks and Wavelet Bases for Rn," *IEEE Trans. on Info. Theory*, vol. 38, no. 2, part 2, pp. 533-555, March 1992. March 1992.

[34] J.-P. Le Cadre, *Contribution a L'Utilisation des Methodes Parametriques en Traitement D'Antenne*, These de Docteur d'Etat Es Sciences, Universite Scientifique et Medicale de Grenoble, France, 1987.

[35] B. F. Logan, "Information in Zero Crossings of Bandpass Signals," *Bell. Syst. Tech. J.*, vol. 56, pp. 487-510, 1977.

[36] P. Maass, "Wideband Approximation and Wavelet Transform," in *Radar and Sonar*, A. Grunbaum. M. Bernfeld and R. Blahut, eds., New York: Springer- Verlag, 1992.

[37] S. Mallat, "Multifrequency Channel Decomposition of Images and Wavelet Models," *IEEE Trans. Acoust. Speech and Signal Proc.*, vol. ASSP-37, pp. 2091-2110, 1989.

[38] S. Mallat, "Zero-Crossings Of A Wavelet Transform," *IEEE Trans. on Info. Theory*, vol. 37, pp. 1019- 1034, July, 1991.

[39] S. Mallat and W. L. Hwang. "Singularity Detection And Processing With Wavelets," *IEEE Trans. on Info. Theory*, vol. 38, no. 2, pp. 617-645, March, 1992.

[40] S. Mallat and S. Zhong, "Characterization Of Signals From Multiscale Edges," *IEEE Trans. PAMI*, vol. 14, no. 7, pp 710-732, July 1992.

[41] B. B. Mandelbrot and J. W. Van Ness, "Fractional Brownian Motions, Fractional Noises and Applications," *SIAM Review*, vol. 10, pp. 422-437, 1968.

[42] Y. Meyer, *Ondelettes et Operateurs*, Paris, France: Herman, 1990.

[43] P. Moulin, J. A. O'Sullivan and D. L. Snyder, "A Method of Sieves for Multiresolution Spectrum Estimation and Radar Imaging," *IEEE Trans. Info. Theory*, vol. IT-38, no. 2, part 2, pp. 801-813, 1992.

[44] H. Naparst, "Dense Target Signal Processing," *IEEE Trans. Info. Theory*, vol. IT-37, no. 2, pp. 317-327, 1991.

[45] A. Paulraj and T. Kailath, "Eigenstructure Methods for Direction of Arrival Estimation in the Presence of Unknown Noise Fields," *IEEE Trans. on Acoust. Speech and Signal Proc.*, vol. ASSP-34, pp. 13-20, 1986.

[46] D. Pollen, "$SU_f(2,F[z.1/z])$ For F a Subfield of C," *J. of the Amer. Math. Soc.*, Vol. 3, no. 3, pp. 611-624, July 1990.

[47] J. P. Reilly and K. M. Wong, "Direction of Arrival Estimation in the Presence of Noise with Unknown Arbitrary Covariance Matrices," in *Proc. of the 1989 Intern. Conf. on Acoust. Speech and Signal Proc.*, Glasgow, Scotland, pp. 2609- 2612, 1989.

[48] A. W. Rihaczek, "Radar Resolution of Moving Targets," *IEEE Trans. Info. Theory*, vol. IT-13, no. 1, pp. 51-56, 1967.

[49] R. O. Schmidt, *A Signal Subspace Approach to Multiple Emitter Location and Spectral Estimation*, Ph.D. Thesis, Stanford University, 1981.

[50] S. Singhal, "High Quality Audio Coding Using Multipulse LPC," *Proc. 1990 Intern. Conf. on Acoust., Speech and Signal Proc.*, pp. 1101-1104, April 1990.

[51] D. Sinha and A. H. Tewfik, "Synthesis/Coding of Audio signals using optimized Wavelets," *Proc. 1992 IEEE Intern. Conf. Acoust. Speech and Signal Proc.*, pp. I-113, San Francisco, CA, March 1992.

[52] D. Sinha and A. H. Tewfik, "Low Bit Rate Transparent Audio Compression Using a Dynamic Dictionary and Optimized Wavelets," in *Proc. of the 1993 IEEE Conf. on Acoust. Speech and Signal Proc.*, Minneapolis, MN, April 1993.

[53] D. Sinha and A. H. Tewfik, "Low Bit Rate Transparent Audio Compression using Adapted Wavelets," to appear in *IEEE Trans. Signal Proc.*, Dec 1993.

[54] D. L. Snyder and H. J. Whitehouse, "Delay-Doppler Radar Using Chirp-Rate Modulation," *10th Colloq. GRETSI*, Nice , France, 1985.

[55] G. Strang, "Wavelets and Dilation Equations: A Brief Introduction," *SIAM Review*, vol. 31, no. 4, pp. 614-627, 1989.

[56] A. H. Tewfik, "Direction Finding in the Presence of Colored Noise by Candidate Identification," *IEEE Trans. Acoust. Speech and Signal Proc.*, vol. ASSP-39, pp. 1933-1942, 1991.

[57] A. H. Tewfik, "Wavelets in Optimal Radar Range-Doppler Imaging," invited paper, in *Proc. 26th Asilomar Conference on Signals, Systems and Computers*, Monterey, CA., Oct. 1992.

[58] A. H. Tewfik, "Waveform Selection for High Resolution Radar Range-Doppler Imaging," Tech. Report, Dept. of Electrical Eng., Univ. of Minnesota, to be submitted to *IEEE Trans. Image Proc.*, April 1993.

[59] A. H. Tewfik, 'Wavelet Domain Bearing Estimation," in preparation, to be submitted to *IEEE Trans. on Signal Proc.*, 1993.

[60] A. H. Tewfik and M. Kim, "Correlation Structure of the Wavelet Coefficients of Fractional Brownian Motions," *IEEE Trans. on Info. Theory*, vol. 38, no. 2, part 2, pp. 904-909, March 1992.

[61] A. H. Tewfik and M. Kim. Fast Multiscale Statistical Signal Processing Algorithms, to appear in *IEEE Trans. on Signal Proc.*, Feb. 1994.

[62] A. H. Tewfik and M. Kim, "Robust Wavelet Domain Array Processing," invited paper, in *Proc. 6h IEEE Signal Proc. Workshop on Statistical Signal and Array Proc.*, Victoria, B. C., Canada, Sept. 1992.

[63] A. H. Tewfik, D. Sinha and P. E. Jorgensen, "On the Optimal Choice of a Wavelet for Signal Representation," accepted for publication, *IEEE Trans. on Info. Theory*, vol. 38, no. 2, part 2, pp. 747-767, March 1992.

[64] P. P. Vaidyanathan, "Multirate Digital Filters, Filter Banks, Polyphase Networks and Applications: A Tutorial," *Proc. IEEE*, vol. 78, no. 1, pp. 56-93, Jan. 1990.

[65] P. P. Vaidyanathan and P. Hoang, "Lattice Structures for Optimal Design and Robust Implementation of Two-Channel Perfect Reconstruction QMF Banks," *IEEE Trans. on Acoust., Speech and Signal Proc.*, vol. 36, pp. 81-94, 1988.

[66] R. N. J. Veldhuis, M. Breeuwer, and R. G. Van Der Waal, "Subband Coding of Digital Audio Signals," *Phillips J. Res*, vol. 44, no. 2-3, pp. 329-343, 1989.

[67] S. Venkataraman and B. C. Levy, "State-Space Representations of 2-D FIR Lossless Matrices and their Application to the Design of 2-D Subband Coders," in *Proc. 25th Asilomar Conference on Signal, Systems and Computers*, Nov. 1991.

[68] M. Vetterli and C. Herley, "Wavelets and Filter Banks: Theory and Design," *IEEE Trans. Signal Proc.*, vol. 40, pp. 2207-2232, Sept. 1992.

[69] M. Vetterli, "Wavelets and Filter Banks for Discrete Time Signal Processing," in *Wavelets and Their Applications*, R. Coifman et al. eds., Jones and Barlett, 1991.

[70] M. Wax "Detection and Localization of Multiple Sources in Noise with Unknown Covariance," *IEEE Trans. on Signal Proc.*, vol. 40, pp. 245-249, 1992.

[71] Y. Yang, K. Wang and S. A. Shamma, "Auditory representation of acoustic signals," *IEEE Trans. on Info. Theory*, vol. 38, no. 2, pp. 824-839, March, 1992.

[72] A. Zakhor and A. V. Oppenheim, "Reconstruction of Two-Dimensional Signals from Level Crossings," in *Proc. IEEE*, vol. 78, no. 1, pp. 31-55, 1990.

[73] H. Zou and A. H. Tewfik, "A Parametrization of Discrete Orthogonal Wavelets," *IEEE Trans. Signal Proc.*, vol. 41, no. 3, pp. 1428-1431, 1993.

[74] H. Zou and A. H. Tewfik, "A Theory of M-band Compactly Supported Orthonormal Wavelets," submitted to *IEEE Trans. on Circ. and Syst.*, Jan. 1992.

[75] H. Zou, A. H. Tewfik and W. Xu , "Completeness and Stability of Partial Wavelet Domain Signal Representations," in *Proc. of the 1993 IEEE Conf. on Acoust. Speech and Signal Proc.*, Minneapolis, MN, April 1993.

[76] H. Zou, A. H. Tewfik and W. Xu, "Signal Reconstruction from a Sampled Dyadic Wavelet Transform Representation," to be *submitted to IEEE Trans. on Signal Processing*, 1993